Spatial and annual variation in fecundity and oocyte atresia of yellowtail flounder, *Limanda ferruginea*, in U.S. waters

W. David McElroy*[12], Mark J. Wuenschel[2], Emilee K. Towle[12], and Richard S. McBride[2]

[1]Integrated Statistics Inc., 172 Shearwater Way, Falmouth, MA 02540 USA
[2]Northeast Fisheries Science Center, National Marine Fisheries Service, 166 Water Street, Woods Hole, MA 02543 USA

*Corresponding author:
Tel.: 00+1+5084952249
Fax: 00+1+5084952258
Email: Dave.McElroy@noaa.gov

Keywords: fecundity; atresia; stereology; down-regulation; geographic variation; condition

Abstract

Potential annual fecundity (PAF) was estimated over three years (2010-2012) for yellowtail flounder with individuals from the three stocks off the northeast U.S. coast. Down-regulation of PAF, the resorption of oocytes during development, was evident as the vitellogenic cohort advanced, so we directly measured atresia of vitellogenic oocytes using stereological techniques. PAF models including relative fish condition, stock area, year, and oocyte diameter of the leading cohort explained more variation than models with just size alone based on Akaike information criteria. In a given year, Gulf of Maine females had lower PAF at size than southern New England females. Interannual differences were evident: PAF of both stocks was higher in 2010 and lower in 2012, with 2011 showing less synchronization between these stocks. Differences in size at age and relative condition suggested that energy available for somatic and reproductive growth was lower in some years in the Gulf of Maine and Georges Bank, especially 2011. Georges Bank PAF and condition were intermediate to the other stocks or more similar to the Gulf of Maine, varying annually. A latitudinal gradient in PAF is evident based on our results and relative to earlier studies that included Canadian stocks. The magnitude of down-regulation was variable across stocks and typically 3-25% of PAF. This can be accounted for in fecundity estimates, by the seasonal schedule of sampling and use of an oocyte diameter term in the fecundity model. Theoretical models of atresia patterns suggested variable rates over the later portion of clutch development. The timing of down-regulation varied among years, and its intensity was influenced by female relative condition. Fecundity was related to fish size, but was also affected by fish condition and oocyte diameter (a proxy for time until spawning), and spatial

52 and temporal effects. A longer time series of PAF may identify environmental drivers that
53 modulate annual stock reproductive potential.

1.0 Introduction

Spawning stock biomass (SSB) is commonly used in fisheries assessments as a proxy for reproductive potential (Saborido-Rey and Trippel, 2013). SSB is generally favored as a proxy because it is relatively easy to calculate from estimates of abundance at age and maturity at age. Given the inherent difficulties in predicting recruitment from SSB, alternative measures of reproductive potential have been proposed (Marshall et al., 2003; Morgan, 2008; Fitzhugh et al., 2012). Direct measures of egg production may be more representative of a stock's reproductive potential because egg production is highly variable; as it is dependent upon dynamic life-history parameters such as maturity, growth, sex ratio, and fecundity, which are all influenced by a fluctuating environment (Rideout and Morgan, 2007; Stares et al., 2007; Lambert, 2013). Alternative measures of reproductive potential can be more responsive to changes in stock demographics and environmental conditions, thereby providing more information to annual stock reproductive potential and subsequent year class strength than biomass metrics alone (Marteinsdottir and Thorarinsson, 1998; Rideout and Morgan, 2010; Lambert, 2013).

Incorporating fecundity and other proxies of reproductive potential into stock assessment models can affect reference points and may improve predictions of year class strength (Morgan et al., 2009; Morgan et al., 2011; Brooks, 2013). Attempts to investigate reproductive potential in an assessment context continue to be constrained by the lack of available data, particularly in the western North Atlantic Ocean where limited stock-specific fecundity data is available (Trippel, 1999; Tomkiewicz et al., 2003). Yellowtail flounder, *Limanda ferruginea*, exemplifies this paucity of data, with few published annual fecundity estimates that are limited in time, geographic scale, or both (Pitt, 1971; Howell and Kesler, 1977; Rideout and Morgan, 2007).

77 Furthermore, of the three stocks in United States waters, annual fecundity has only been
78 estimated for the southern New England stock (Howell and Kesler, 1977).
79 Oocyte development in yellowtail flounder is group synchronous (Howell and Kesler
80 1977; Howell, 1983) with a distinct cohort of maturing (secondary growth) oocytes leading up to
81 spawning, hence fecundity is determinate. The estimation of the number of oocytes in this
82 maturing cohort – referred to here as the potential annual fecundity (PAF) – can be partially
83 automated by image analysis systems, using the autodiametric method (Thorsen and Kjesbu,
84 2001; Witthames et al., 2009; Ganias et al., 2014). The autodiametric method estimates oocyte
85 density (number of oocytes / g ovary, NG) from the mean diameter of secondary growth oocytes
86 (i.e. the developing cohort), facilitating measurement of fecundity, but has not yet been applied
87 to yellowtail flounder, so we determined this relationship.
88 Many fish 'fine-tune' their annual fecundity as the clutch develops. Therefore, estimates
89 of PAF should be measured as close as possible, but prior, to spawning so that PAF estimates are
90 considered the best approximation of realized annual fecundity (RAF; Murua et al., 2003; Ganias
91 et al., 2014), defined as the actual number of eggs released. Differences between PAF and RAF
92 can arise when atresia of developing oocytes reduces the standing crop of secondary-growth
93 oocytes (termed down-regulation) or when the entire clutch, or portions of, is not released,
94 evidenced by residual eggs in the spent ovary (Kurita et al., 2003; Murua et al., 2003). Both
95 atresia and residual eggs have been noted in yellowtail flounder (Howell, 1983; Zamarro, 1991);
96 hence, we sought to quantify annual rates of atresia using a Weibel grid stereological procedure
97 (Weibel et al., 1966; Weibel, 1979; Sterio, 1984), as applied to fecundity analysis (Emerson et
98 al., 1990; Andersen, 2003).

In this study we estimated female yellowtail flounder fecundity during three spawning seasons, 2010-2012, among the three stocks in U.S. waters: Gulf of Maine (GOM), Georges Bank (GB), and Southern New England-Middle Atlantic (referred herein simply as SNE, the only sub-region we obtained samples from). The Georges Bank stock is a shared stock with Canada, and only the U.S. portion of the stock was sampled. Determination of both fecundity and atresia allowed us to assess the scale, timing, and spatiotemporal variation in down-regulation during the development of the annual clutch. Data on the reproductive output of yellowtail flounder are especially relevant in light of the current low levels of biomass and recruitment in the SNE and GB stocks (NEFSC, 2012a, 2012b; Legault et al., 2013).

2.0 Methods

Yellowtail flounder were sampled monthly from January 2010 through June 2011, and in 2012 sampling was narrowed to just the three months prior to peak spawning for each stock. Fish were collected primarily by commercial fishing vessels participating in the Northeast Fisheries Science Center, Northeast Cooperative Research Program's (NEFSC-NCRP) Study Fleet (n = 310 females) and from other NEFSC-NCRP research studies (n = 56). Fishermen were paid to provide a subset of 30-40 random fish distributed over the size range captured, and depending on the catch volume this was typically from one or two hauls. The fishermen tracked which haul the fish were from, along with the location and time of the haul, using electronic fisheries logbook software used for catch reporting. To ensure a high quality of the tissues, fish were requested from the last day (or tows) of a fishing trip, iced during transport, and processed upon arrival at the laboratory. Supplemental samples were acquired from the Massachusetts Division of Marine Fisheries trawl survey (n = 21) and NEFSC bottom trawl survey (n = 23). Two fish per 1 cm bin

were randomly selected on the NEFSC survey, and all developing fish observed on a tow were selected for the MADMF survey. Both surveys have a random stratified survey design. Fish were obtained from core areas of abundance, and the sizes were representative for all three stock areas in United States' waters (Fig. 1; Table 1). Fish total length (TL, mm), body mass (M_b, $\pm$ 0.1 g), and ovarian mass (M_o, $\pm$ 0.001g) were measured, and an approximately 1 cm^3 piece of tissue from the middle of the right ovarian lobe was fixed in 10% neutral-buffered formalin. A few fish were sampled while at sea (TL $\pm$ 0.5 cm, M_b and M_o $\pm$ 0.001 kg, n = 44).

Age was determined for each fish by counting annuli on scale impressions following methods developed at the NEFSC, which are used in the three stock assessments (NEFSC, 2012a, 2012b; Legault et al., 2013). Specifically, about 5 or 6 scales from the eyed side along the lateral line were impressed on a laminated plastic slide using a roller press and viewed on a microprojector at a magnification of 52X with transmitted light (Penttila & Dery 1988). Details on ageing methods and quality control/quality assurance procedures and results are available at http://www.nefsc.noaa.gov/fbp/.

2.1 Relative condition

Relative condition (K_n) was calculated as the ratio of the observed mass over the predicted body mass (Le Cren, 1951) using an overall length-mass equation determined from all females sampled for fecundity. This was calculated using a log-transformed least squares regression: $LN(M_{ofb}) = -11.364 + 2.934\ LN(TL)$, ($n$ = 410, SE a = 0.271, SE b = 0.046, r^2 = 0.91). Ovary-free body mass M_{ofb} was used to examine changes in condition independent of ovarian development. Differences in K_n among stocks and years were tested by ANOVA with a

144 Tukey HSD post-hoc test if overall significant differences were found. This and all subsequent
145 statistical analyses were performed using R version 3.0.1 (R Development Core Team, 2013)[1].
146
147 2.2 Histology
148 The fixed ovarian tissue was processed with standard histological methods to assess
149 microscopic characteristics of fish gonads. Samples were embedded in paraffin blocks, thin
150 sectioned, and stained with Schiffs-Mallory trichrome (SMT). The most advanced oocyte stage
151 (MAOS), the presence of postovulatory follicles, and the occurrence and stage of atresia were
152 assessed for each histology section. The MAOS scheme was adapted from previous studies of
153 this species (Howell, 1983; Zamarro, 1991) and Lowerre-Barbieri et al. (2011), which includes
154 the following classifications; primary growth (all oocyte stages prior to cortical alveolar),
155 cortical alveolar, early vitellogenic (partially yolked), late vitellogenic (fully yoked), germinal
156 vesicle migration, germinal vesicle breakdown, hydration, and ovulation. Fecundity analysis
157 included only females with a MAOS in late vitellogenesis or germinal vesicle migration.
158 Females were excluded if there were signs of spawning activity (germinal vesicle breakdown,
159 hydrated oocytes, or postovulatory follicles) or any indications of significant cell damage (e.g.,
160 due to freezing, which occasionally occurred during transit to the laboratory).
161 Atresia was classified as either α or β atresia based on criteria adapted from Hunter and
162 Macewicz (1985) and Witthames and Greer Walker (1995). The α stage was first evident by
163 distortion and fissures in the zona pelucida (Fig. 2). As the α stage progressed the zona pelucida
164 fragmented and collapsed toward the center of the cell, the germinal vesicle disintegrated, and
165 yolk globules disappeared as they were phagocytized and the oocyte became vacuolated in

[1] Mention of this or any other products is for descriptive purposes and does not indicate endorsement by the National Marine Fisheries Service.

166 appearance. The α stage was considered complete when the zona pelucida and distinct yolk
167 globules were no longer evident. The β stage was more compact and irregular in shape with
168 numerous vacuoles that were either empty or contained particles of the phagocytized material.
169
170 2.3 Fecundity determination
171 Direct gravimetric measurements of oocyte density were made from subsamples of the
172 fixed ovarian tissue, without any tunica tissue (gonad wall), that were patted dry, and weighed (±
173 0.0001g). A subsample of 300-400 oocytes was targeted to balance sample size with processing
174 time. Subsamples were manipulated with probes to separate the individual oocytes into a single
175 layer, and images were taken with transmitted light using a dissecting scope and digital camera
176 (1.5X). ImageJ software[2] (v. 1.46r, National Institute of Health) and the ObjectJ (v. 1.02k,
177 University of Amsterdam) plugin were used for image processing. All images were evaluated on
178 a qualitative scale (good = 1, adequate = 2, poor = 3), which were graded based on the clarity of
179 images, amount of oocytes damaged from processing, and quantity of connective tissue clinging
180 to oocytes. Samples with poor quality (3) were excluded from subsequent analyses, and a new
181 subsample was processed (n = 4). Analysis of images was made consistent between samples by
182 use of a macro in ObjectJ, modified from one developed for Atlantic mackerel, *Scomber*
183 *scombrus* (Dr. Anders Thorsen, Institute of Marine Research, Bergen, Norway, pers. comm.).
184 The macro automatically filtered the images and measured the oocyte diameters. Subsequent
185 inspection of the processed image allowed correction of erroneously identified and measured
186 particles (e.g., connective tissue, or oocytes adhering to each other but not identified as separate
187 objects). To avoid potential size bias, the diameters of oocytes damaged during sample

[2] Mention of this or any other products is for descriptive purposes and does not indicate endorsement by the National Marine Fisheries Service.

188 processing were not included in the estimation of the mean, but the number of damaged cells was
189 included in the total oocyte count for the subsample (number of oocytes/g of ovary, NG) in
190 gravimetric subsamples. These gravimetric estimates were used to determine the autodiametric
191 relationship between mean oocyte diameter and oocyte density, and oocyte density was
192 estimated for all subsequent fish using their mean oocyte diameter.
193 To ensure individual fish were at an appropriate development stage for fecundity
194 analysis, the size distribution of measured oocytes for each fish was assessed with the following
195 two criteria to remove individuals too early in development. These criteria also reduced the
196 impact of stock differences in spawning seasonality. The first criteria verified that the
197 vitellogenic cohort of oocytes for the imminent spawning season had achieved a clear hiatus
198 from the reservoir of smaller primary growth oocytes, from which subsequent cohorts would
199 emerge in future years. Specifically, if > 5% of the measured vitellogenic oocytes had an oocyte
200 diameter that was smaller than 250 μm, then the individual was excluded (see electronic
201 supplementary materials Fig. S.1). The second threshold confirmed the leading cohort (largest
202 10% of oocytes) had reached a minimum size threshold of development. Specifically, individuals
203 with a leading cohort < 375 μm were considered too early in development and excluded. These
204 thresholds were determined by examination of oocyte length-frequency distributions and ovarian
205 histology, which identified the size break between partially and fully vitellogenic (~250 μm)
206 oocytes and those approaching the end of vitellogenesis (~375 μm) but prior to germinal vessel
207 migration.
208 To confirm that samples from a single ovarian location were representative of the entire
209 ovary, we measured oocyte density and mean oocyte diameter for samples from multiple gonad
210 locations within and between ovarian lobes for 10 females. For these individuals, six samples of

211 tissue were taken, one each from the anterior, middle, and posterior of each ovarian lobe and
212 processed as described above. To account for individual differences in developmental stage
213 among fish, a mixed model with individual fish as the random effect was used to evaluate
214 whether the two response variables differed among the six ovary locations (McElroy et al., 2013;
215 used lme function of the nlme package in R). Although there was significant variation in oocyte
216 diameter among fish (the random effect), no significant difference in oocyte diameter (DF = 45,
217 p's = 0.24 - 0.82) or oocyte density (DF = 45, p's = 0.17 - 0.60) was detected between samples
218 from the same individual (see electronic supplementary materials Fig. S.2). Therefore, a sample
219 from one location, generally the middle of the dorsal lobe, was considered representative of the
220 entire ovary.

221 The autodiametric relationship, oocyte density (NG) as a function of the mean oocyte
222 diameter (OD), was modeled with both power and exponential functions using least-squares
223 regression. The best model was selected using second order Akaike information criterion, AICc
224 (Anderson, 2008; AICctab function from bbmle package in R). The power model fit the data
225 better than the exponential model (n = 178, ΔAICc = 6.3). The fitted equation used for
226 determination of the oocyte density based on the gravimetric samples was $NG = (5.919x10^{10})$
227 $(OD^{-2.446})$; subsequently, (see electronic supplementary materials Fig. S.3; n = 178, SE a =
228 $3.033x10^{10}$, SE b = 0.086; OD range = 324 – 514 μm) this model was used to calculate the
229 oocyte density for the additional 232 females (OD range = 324 – 509 μm) used in all the
230 following analyses.

231 When scaling up the oocyte density (NG) of the subsample to estimate the fecundity of a
232 whole fish; we adjusted for the tunica's contribution to the whole ovarian mass (M_o). To do so,
233 the tunica weight was determined by weighing the whole wet ovary initially and then stripped of

all oocytes. Tunica mass expressed as a percentage of whole ovarian mass (4.721%, n = 57, SE = 0.169) was used to adjust M_o for calculation of PAF as follows: PAF = NG (0.9528 M_o), where NG (oocytes/g) was either measured gravimetrically or calculated with the autodiametric curve.

2.4 Fecundity modeling

We modeled PAF as a function of fish size (TL) or age (FA) by: ln(PAF) = β_1 ln(TL or FA) + α, where α and β_1 are coefficients determined by least-squares fit regression. Fish TL was used as the measure of fish size as the total mass of fish is dynamic leading up to spawning. Total fish mass increases as the annual clutch develops due to the gonad weight increasing, but gonad-free fish mass concurrently declines as fish deplete somatic energy reserves. Since fish were sampled over a relatively broad period leading up to spawning, TL was chosen to describe fish size as it is more stable. Age models were tested and age-PAF relationships were reported, but model analysis was only presented for length as it related more strongly to PAF. Model selection evaluated the inclusion of stock and year as factors, and relative condition (K_n) and mean oocyte diameter of the leading cohort (OD_{LC}) as continuous variables. Models including all combinations of main effects were evaluated – from simple individual predictor models to a model with all main effects combined – using AICc criteria (using dredge function in the MuMIn package of R). Interaction terms were also evaluated, but most produced little improvement over models with main effects only (ΔAICc < 2). Parsimony lead us to avoid tabulating statistics of all models with interaction terms, except for models with stock:year and stock:age interactions. Since the AIC approach can select the best among even poor models, the coefficient of determination (r^2) was also calculated to evaluate model fit.

256 The numbers and lengths of fish sampled varied among stocks, and to a lesser degree
257 years (Table 1). The differences in size among stocks reflected established patterns in growth,
258 but also the variable nature of the maximum and minimum lengths encountered. Variation in
259 numbers of fish collected was influenced by seasonal fishing patterns and available quota for the
260 participating fishermen. In particular, samples from the GB stock were excluded from most
261 analyses due to low sample size and a narrow length range. Therefore, PAF model testing was
262 limited to a range of lengths that overlapped for females sampled from the SNE and GOM stocks
263 in all years, rounded to the nearest cm (33 – 45 cm TL [n = 338]). Two fish collected in the
264 month of December were grouped with the subsequent calendar year in which they would have
265 spawned. The form of the final reported PAF regressions was determined based on the model
266 testing, and slopes of the final regressions were tested against an isometric slope (β_1 = 3 for
267 length, β_1 = 1 for age) using a Wald test.
268
269 2.5 Down-regulation analyses
270 Two complimentary approaches (across and within individuals) were used to quantify the
271 magnitude of down-regulation of fecundity for the stocks studied. First, we inspected trends in
272 PAF over the period of the oocyte development cycle covered by all fish sampled for fecundity
273 (population level, across point estimates from individuals) as an indirect measure of down-
274 regulation. Second, for a subset of individuals we assessed combined (alpha and beta)
275 vitellogenic atresia at the individual level using stereological methods to directly quantify the
276 percentage of atretic oocytes present.
277
278 2.5.1 Down-regulation via PAF estimates

279 The relationship between PAF estimates and mean leading cohort diameter, OD_{LC} (a
280 proxy for time to spawning) was used to evaluate if fecundity estimates declined as spawning
281 approached (i.e. down-regulation). Stock- and year-specific regressions were used to generate
282 length-based residuals for PAF estimates (all years combined for GB regression), which were
283 standardized to predicted PAF (pPAF). K_n was included in the models for determining pPAF, but
284 mean OD_{LC} was not included to maintain independence in the subsequent regression analysis
285 relative to OD_{LC}. Ten fish were omitted from the regressions because they had rare lengths (TL <
286 300 mm or TL > 500 mm) or ages (2 years). The linear regression of the standardized PAF-
287 residuals against mean OD_{LC} was then tested to determine if the slope differed from zero (no
288 down-regulation).
289
290 2.5.2 Down-regulation via stereological estimates
291 A subset of fish was selected from the fecundity samples for direct estimation of atresia
292 using stereological analysis of ovarian histology. We adapted methods developed by Weibel et
293 al. (1966) and Sterio (1984), and as applied to fish reproduction by Emerson et al. (1990) and
294 Andersen (2003) to quantify the relative intensity of atresia of secondary-growth oocytes. This
295 method provides unbiased estimates of volume fraction of different cell types from two
296 dimensional cross sections. Fish were randomly selected from 50 μm intervals (< 350, 350 – 400,
297 400 – 450, > 450 μm mean oocyte diameter) as sample availability allowed (n = 27, 51, 44, 42;
298 respectively), while maintaining a balanced representation across stock and year (n = 20 per year
299 for GOM and SNE; but only n = 9, 17, and 18 were available for GB in 2010-2012). Serial, non-
300 overlapping images were captured from one histology section (per fish) at 4X magnification on a
301 compound microscope. A 0.1815 cm x 0.1312 cm grid, containing 120 sampling points (Fig. 2;

302 Weibel 1979; Sterio 1984; Andersen 2003), was overlaid on each image using the Weibel grid
303 macro in ObjectJ (see section 2.2).

304 The number of sampling points hitting each cell type (vitellogenic oocytes, α and β stages
305 of atresia) and total number of cells transected by the grid were enumerated for each image. If
306 cells were found entirely within the borders of the grid or crossed the top and right 'allowed'
307 borders (Fig. 2) they were counted; cells outside the grid or crossing the 'forbidden' (left or
308 bottom) borders were not counted. White space in the images was recorded as negative sampling
309 points, and excluded from the calculations of volume fraction (below). Similarly, tunica tissue
310 was recorded and excluded from the calculations as it was not included in fecundity subsamples.
311 The number of images used for each fish depended on the size of the histology section, which
312 varied with the stage of ovarian development. Therefore, a target was set at 300 vitellogenic
313 oocytes (mean = 315 oocytes), and fish with less than 200 transections were excluded from the
314 analysis.

315 The count data from the two dimensional histology micrographs was converted to a three
316 dimensional estimate of density (N_v, number per unit volume) by the following equation for the
317 i^{th} cell type (vitellogenic [N_{vv}], α-atretic [$N_{v\alpha}$], or β-atretic [$N_{v\beta}$]):

318 Eq. 1 $$N_{vi} = \frac{K \cdot N \cdot}{\beta \cdot V^{0.}},$$

319 where N_{ai} is the number of oocytes per unit area for cell type i, V_i is the volume fraction occupied
320 by cell type i, β is a shape coefficient, and K is a size distribution coefficient (Weibel et al.,
321 1966). N_{ai} was calculated as the number of oocyte profiles transected per unit area for each cell
322 type. The grid area (0.0238 cm^2) was multiplied by the number of images (N_m) for each fish to
323 get the total area sampled. For each fish, V_i was determined for each cell type using:

324 Eq. 2 $$V_i = \frac{\sum_{m=}^{n} P_m}{(120 \cdot N_m - P_n)},$$

where P_{im} is the number of sampling points hitting cell type i in the m^{th} image, 120 is the total number of sampling points per grid, and P_n is the total number of negative sampling (and tunica) points observed for that fish.

The coefficients β and K were determined from diameter measurements taken from the histology for a subset of 20 fish, from which 50 vitellogenic oocytes per fish (total n = 1000 oocytes) were measured and as many α- (n = 269) and β-atretic (n = 273) oocytes as were available. Different coefficient values were used for each cell type since vitellogenic oocytes were relatively spherical in shape, but α and β atresia were more irregular in shape and varied dependent on the amount of cellular breakdown that had occurred. The coefficient β was calculated as the ratio of the longest to the shortest axis for each cell type (Weibel and Gomez, 1962; Emerson et al., 1990). A value of β_v = 1.3091 was determined for use with vitellogenic cells, and higher values of β_α = 2.0440 and β_β = 2.5058 were determined for the α- and β-atretic oocytes, respectively. K was determined using the equation: $K = (M_3/M_1)^{1.5}$, where M_1 and M_3 are the first and third moment of the size distribution (Weibel et al., 1966). The cell specific values of K were: 1.0113 for vitellogenic cells, 1.1133 and 1.1468 for α and β atresia, respectively.

The relative intensity of atresia was estimated as a percentage of total secondary growth oocytes for α ($\%A_\alpha$) and β atresia ($\%A_\beta$) separately and for combined atresia ($\%A_c$) as follows: $\%A_c = 100\ (N_{v\alpha} + N_{v\beta}) / (N_{vv} + N_{v\alpha} + N_{v\beta})$. The $\%A_c$ was compared using simple linear regression to both mean OD_{LC} and K_n. Differences in K_n between stock-year combinations, excluding GB (due to low sample size), were tested using ANOVA on the arcsine square-root transformed proportion A_c.

348 2.5.3 Theoretical down-regulation models

349 In an effort to explore the ramifications of the observed point estimates of down-
350 regulation, we developed theoretical models of atretic down-regulation patterns for yellowtail
351 flounder over the oocyte development period, i.e. the measured OD_{LC} range. Several theoretical
352 patterns of down-regulation were considered, a low and steady rate (constant 2% atresia), a
353 single acute event (one brief period of 10% atresia), an episodic pattern (two periods of 2% and
354 one of 5% atresia), and a variable rate (longer periods of 0-3% and episodic 4-7% atresia).
355 Probability density functions (PDF) were applied to each potential model and scaled to the
356 observed distribution of relative fecundity for yellowtail flounder. Relative fecundity (oocytes / g
357 of gonad-free female) was used to control for the effect of female size, and one extreme relative
358 fecundity value (>7.6) was excluded to facilitate comparison among the theoretical models.
359

360 **3.0 Results**

361 3.1 Fecundity modeling

362 AICc values indicated length was the best single predictor model for PAF (Table 2a),
363 explaining 62% of the variation in PAF. Adding other predictors was found to improve the
364 model, and the model with the lowest AICc included all five main effects and the one interaction
365 term (Table 2b). All potential combinations of main effects and the one interaction were tested,
366 but for simplicity only the best models for each number of parameters are shown. The best two
367 parameter model added K_n to TL, increasing the explanatory power to 71%. Additional
368 parameters increased the explanatory power of the model incrementally, with the final model
369 explaining 80% of the variation in PAF.

370 The increase in PAF in relation to length had significant positive allometry for both SNE
371 and GOM females ($\beta_1 > 3$), for stock specific regressions of all years combined (Table 3; Fig. 3).
372 This was not the case for the GB females sampled, which was likely an artifact of the low data
373 density over the length range. Fecundity at age exhibited greater variation than fecundity at
374 length (Table 3). The increase in PAF in relation to age was significantly lower than the null
375 slope (slope = 1) for GOM females, but not so for individuals from SNE indicating slower
376 increases in PAF with age in GOM compared to SNE. The interannual and stock differences in
377 PAF models at age were consistent with the patterns in length at age among years and stocks
378 (Fig. 4).
379 Model estimates of PAF at length or age were higher for females from SNE than those
380 from the GOM within all years (Fig. 4). Graphical comparisons of estimates were standardized
381 by setting relative condition at 1.0 ('average condition') and the leading cohort diameter at 500
382 μm. Comparison across years of the individual data points indicated substantial overlap among
383 the stocks (Fig. 3). This overlap was particularly evident in 2010, the year with the highest PAF
384 estimates for GOM females, which were comparable with the estimates in the lowest year for
385 SNE females, 2012 (Fig. 4). Trends in PAF were synchronized across stocks in two of the years,
386 with both GOM and SNE exhibiting high PAF in 2010 and low PAF in 2012. However, in 2011,
387 PAF estimates were not synchronized as the PAF estimates of SNE fish were high, similar to
388 2010 SNE fish; whereas GOM 2011 estimates were low, similar to 2012 GOM fish. The
389 explained variation (r^2) in PAF was also higher for all the SNE regressions relative to the GOM
390 models, for both length and age (Table 3). Among years the model estimates of GOM fecundity
391 at both length and age also exhibited greater variation than SNE PAF (Fig. 4a, b).

392 The sample size and length range of fish from GB were too low to include in the model
393 analysis (Table 3; Fig. 3), but the patterns in the available data suggested fecundity of this third
394 stock was intermediate to the other two stocks or closer to the lower values observed in GOM,
395 differing annually. The low fecundity estimates for GB fish in 2011 corresponded with the very
396 low values of relative condition observed for GB fish in 2011 (Fig. 5). Condition of GB females
397 had the highest slope relative to fecundity of any stock (Table 3). These results for GB females
398 are tentative, drawn from highly variable estimates of PAF, and a narrow size range of fish
399 sampled.
400
401 3.2 Relative condition
402 Relative condition varied significantly overall among stocks and years for the SNE and
403 GOM stocks (Fig. 5; $F = 9.746$, $n = 356$, $p < 0.01$), and contributed to explaining variation in the
404 length-PAF models (Table 2). In post-hoc testing, the K_n of females for two stock-year
405 combinations were significant (Tukey HSD, $p < 0.05$). The K_n for SNE in 2011 was significantly
406 greater than the K_n for GOM in all years. The K_n for GOM in 2011 was significantly lower than
407 all other stock-year combinations. Relative condition had a significant positive, but weak,
408 relationship to standardized PAF residuals (Fig. 6a; slope = 99.77, $n = 400$, $r^2 = 0.13$, $p < 0.01$).
409 PAF residuals were determined with stock-year specific regressions (except GB which was all
410 years combined) with a mean OD_{LC} term. Individuals with very high or low condition were
411 associated with higher or lower fecundity than expected at a given length. The particularly low
412 K_n for GOM fish sampled in 2011 was associated with low PAF, and high condition of SNE fish
413 in 2011 with higher fecundity (Fig. 4, 5). However, at a stock level, condition was not always
414 directly predictive of variation in fecundity for a given year (i.e. 2012 fecundity and condition).

415

416 3.3 Down-regulation of fecundity

417 Results from the two independent approaches indicated low levels of down-regulation
418 occurred during the sampling period. All OD_{LC} regression terms in the PAF models had negative
419 slopes – except SNE in 2010 FA model (Table 3), an indirect indicator of down-regulation,
420 which were consistent with the decline in standardized PAF residuals as mean OD_{LC} increased
421 (Fig. 6b). The declining slope of the regression for PAF residuals with OD_{LC} was significant
422 (slope = -0.103, n = 400, r^2 = 0.04, $p < 0.01$), but the strength of the relationship was extremely
423 weak. To examine interannual patterns in down-regulation, stock-year specific PAF regressions
424 were used, and PAF for a given length (400 mm) and condition (K_n = 1) was predicted at two
425 OD_{LC}'s within the range examined. Predicted PAF declined from 3-25% as the mean OD_{LC}
426 advanced from 400 to 500 μm for all stocks and years (Table 4). Higher rates of down-regulation
427 were observed for GOM (8-25%) than SNE (3-13%) and GB (8%) females, and rates were
428 highest for GOM and SNE in 2011.

429 In terms of the direct measure of down-regulation, mean stereological estimates of the
430 relative intensity of combined atresia (α and β) were generally low, $A_c < 5\%$, for the majority of
431 individuals; although some fish did have levels exceeding 10% (Fig. 7a). There was no apparent
432 trend in $\%A_c$ across the range of OD_{LC}'s sampled (slope = -0.002, n = 164, $r^2 < 0.01$, p = 0.84).
433 Looking separately at the two atresia types, β atresia was consistently 1-2% higher than α atresia,
434 but neither measure was significantly related to mean OD_{LC} ($\%A_\alpha$: slope = -0.003, n = 164, $r^2 <$
435 0.01, p = 0.47; $\%A_\beta$: slope = 0.001, n = 164, $r^2 < 0.01$, p = 0.88). Some fish with low condition
436 did exhibit high $\%A_c$ and most of those with high condition exhibited low $\%A_c$ (Fig. 7b). The
437 quantity of atresia was highly variable across the range of observed conditions resulting in a

438 weak relationship; however, the negative slope of the regression was significant (slope = -
439 15.563, n = 164, r^2 = 0.06, p < 0.01).

440 At a stock level, the direct measures of the individual intensity of atresia varied within
441 and among the stocks. The SNE fish had the lowest $\%A_c$ of all the stocks, generally < 3%;
442 whereas GOM females had a broader interquartile range (0-5%A_c; Fig. 8). The more limited
443 samples of fish from GB had the highest individual atresia levels and exceeded 5%A_c more
444 frequently than the other stocks. Interannual differences were limited, but $\%A_c$ was generally
445 very low in 2010 for fish from all 3 stocks, especially relative to fish sampled in 2011. However,
446 the proportion A_c was not significantly different among years for yellowtail flounder from GOM
447 and SNE (F = 1.835, n = 120, p = 0.11).

448 The theoretical model for down-regulation with a relatively constant atretic rate produced
449 a PDF that was similar to but not entirely consistent with the observed PDF (Fig. 9). Single acute
450 and episodic patterns of atresia were multimodal with little similarity to the observed PDF. A
451 variable pattern with periods of low steady and brief higher intensity atresia produced a PDF
452 more similar to that of the observed data.

453

454 **4.0 Discussion**

455

456 4.1 Size- and age-dependent fecundity

457 Yellowtail flounder size (length) was the best predictor of PAF, and PAF increased with
458 both increasing length and age. We chose length as a metric of size rather than fish mass because
459 even gonad-free fish mass changes in relation to length seasonally due to storage and or
460 depletion of energy reserves (Skjæraasen et al., 2006; Alonso-Fernández et al., 2009; McElroy et

461 al., 2013). Samples were representative of the lengths and ages occurring in the commercial
462 catch presently, but may not precisely reflect their relative abundance (NEFSC, 2012a, 2012b;
463 Legault et al., 2013). Age was a weaker predictor than length, which may be partially attributed
464 to the observed differences in size at age among years and stocks. This was particularly true for
465 the GOM fish, which grow slower than SNE fish (NEFSC 2012a). Howell and Kesler (1977)
466 also reported that length was more predictive of fecundity than age for yellowtail flounder.
467 The positive allometry ($\beta_1 > 3$) in the relationship between fecundity and size indicates
468 greater egg production by large females than expected based on their size alone. Earlier
469 yellowtail fecundity studies by Pitt (1971) and Howell and Kesler (1977) included larger fish up
470 to 54 cm TL and reported higher slopes than the current study ($\beta = 4.69$ and 3.86, respectively).
471 Because U.S. stocks of yellowtail flounder have experienced truncated size and age structure for
472 a decade or more (NEFSC, 2012a, 2012b; Legault et al., 2013), it is likely they are capable of
473 higher fecundity at size than reported here as few fish sampled were larger than 45 cm. The
474 increased relative fecundity for larger females, as shown in other species (Wootton, 1990),
475 indicates that both SSB and stock demographics determine stock reproductive potential.
476 Additional data from larger fish would help quantify the value of these larger fish to overall
477 stock productivity.
478 We only examined patterns in potential fecundity and were not able to assess realized
479 fecundity or variation in egg size or quality. Greater egg size, which generally confers higher
480 survival to larvae, has been related to maternal size or age in some species including: Atlantic
481 cod, *Gadus morhua* (Kjesbu et al., 1996), haddock, *Melanogrammus aeglefinus* (Trippel and
482 Neil, 2004), plaice, *Pleuronectes platessus* (Kennedy et al., 2007) and winter flounder,
483 *Pseudopleuronectes americanus* (Buckley et al., 1991). Experimental studies on maternal effects

484 in yellowtail flounder are equivocal; Manning and Crim (1998) found no relationship between
485 egg size and egg dry weight with maternal size, while Benoît and Pepin (1999) report strong
486 maternal effects on larval hatch size, but the sample sizes were small in both studies. Further
487 research is necessary to understand maternal effects for yellowtail flounder; as both fecundity
488 and the size and quality of propagules contribute to reproductive potential.
489
490 4.2 Between stock variation in fecundity
491 Our study applied a single method across the stocks and demonstrated both between and
492 within stock variation of yellowtail flounder fecundity in U.S. waters. Model estimates of PAF
493 were higher for SNE females, relative to GOM fish, within all years. Although only 200 km
494 separates these collection areas, they are bisected by Cape Cod, which demarcates a major
495 zoogeographic boundary (Briggs, 1974). Our sampling covered much of the current high
496 abundance areas of the yellowtail population in U.S. waters (NEFSC, 2012a, 2012b; Legault et
497 al., 2013), and likely captured much of the variation in fecundity that presently exists in U.S.
498 waters. However, we did not sample yellowtail flounder farther south, along the middle Atlantic
499 bight, a region where their abundance has declined recently.
500 Spatial variation in fish fecundity is common in other groundfishes (Blanchard et al.,
501 2003; Cooper et al., 2007; Witthames et al., 2013). In the sympatric winter flounder,
502 *Pseudopleuronectes americanus*, fecundity was also lower for individuals from the GOM
503 compared to the SNE stock, with comparable spatial scale in sampling (McElroy et al., 2013).
504 Populations in these two regions, for both flounder species, are considered separate stocks. In the
505 case of winter flounder, several phenotypic traits, including growth which influences fecundity,
506 are consistent with genetic differentiation between SNE and GOM (DeCelles and Cadrin, 2011;

507 Wirgin et al., 2014); however, genetic studies have provided inconclusive evidence for
508 yelllowtail flounder stock structure (Cadrin, 2010). Genetic structuring may be reduced for
509 yellowtail flounder due to greater dispersal and mixing of pelagic eggs as compared to the
510 benthic winter flounder egg. Spatial variation in yellowtail flounder fecundity has been identified
511 in Canadian waters (Rideout and Morgan, 2007), but interstock variation in yellowtail flounder
512 fecundity within U.S. waters had not been previously described.

513 There may be stock-specific differences between the coastal stocks (SNE, GOM) and the
514 transboundary offshore stock (GB) as well; spawning stock biomass at age is known to vary by
515 stock for yellowtail flounder in the US due to differences in maturity and weight at age (NEFSC,
516 2012a, 2012b; Legault et al., 2013). However, sample size of the GB stock was too low and the
517 variability of the estimates was high, which prevented us from including them in the present
518 comparative analyses. Qualitatively, estimates of PAF for females from GB were more aligned
519 with the lower fecundity evident in GOM than with SNE individuals, and this was consistent
520 with low levels of K_n and higher levels of $\%A_c$ observed for GB females, in the years studied. It
521 is possible that the low somatic condition of this stock in recent years (Legault et al., 2013),
522 particularly in 2011, has contributed to more variable and lower fecundity. Further sampling of
523 this stock is necessary understand its reproductive dynamics, the importance of which is
524 magnified by the current low abundance of the stock and record low recruitment (Legault et al.,
525 2013).

526 Our fecundity at length estimates are higher than previous reports for yellowtail flounder
527 in the northwestern Atlantic Ocean (Table 5), particularly for SNE individuals (Howell and
528 Kesler, 1977). Pitt (1971) in the 1960's, and more recently Rideout and Morgan (2007) reported
529 lower yellowtail PAF for Grand Bank yellowtail than observed in U.S. waters. This later study

530 also found lower fecundity for females on the eastern side (3LNO NAFO region) of the Grand
531 Bank than the western portion (3Ps). At a greater spatial scale than just the present study,
532 fecundity in the GOM is intermediate between that for Grand Bank and SNE, further supporting
533 a latitudinal trend. Evidence for this latitudinal trend in yellowtail flounder fecundity was first
534 identified by Howell and Kesler (1977), who compared their estimates for SNE to reported
535 fecundity from the Grand Bank (Pitt, 1971). Cross study comparisons in fecundity are
536 complicated by temporal separation differences in methodology, and the lack of a common
537 minimum oocyte size-threshold. The earlier studies covered a similar overall oocyte diameter
538 range to the present work, but those studies may have included more fish with low mean oocyte
539 diameters and so lower cumulative down-regulation, resulting in higher estimates of fecundity at
540 length. However, results within the current study and collectively with earlier work and the
541 multiple Grand Bank studies provide support for decreasing fecundity with increasing latitude as
542 has been demonstrated in other species and regions (e.g. Thorsen et al., 2010).
543
544 4.3 Within stock variation in fecundity
545 Interannual differences in fecundity were evident in both coastal stocks and were
546 synchronous in two of the three years sampled, 2010 (both higher) and 2012 (both lower).
547 Similarly, down-regulation was highest in 2011 for both the GOM and SNE stocks. Interannual
548 variations in fecundity has frequently been related to environmental conditions, feeding, or both
549 (Horwood et al., 1989; Skjæraasen et al., 2006; Kjesbu and Witthames, 2007; Morgan et al.,
550 2010), therefore synchrony across stocks in certain years may indicate larger scale (regional)
551 forcing of environmental conditions. However, PAF was not synchronized among regions in all
552 years (i.e. 2011). On the Grand Bank, Rideout and Morgan (2007) also reported interannual

553 variation in fecundity at length between years in the 1990s and even greater differences with
554 estimates from the 1960's (Pitt, 1971). Our estimates of fecundity at length for SNE individuals
555 are higher than earlier studies (Table 5). Continued sampling over a longer timescale is necessary
556 to fully characterize the level of PAF synchronization among the yellowtail flounder stocks,
557 temporal dynamics, and assess linkages to potential driving factors.
558 Within-stock spatial variation in reproductive output of yellowtail flounder may also exist
559 but was not investigated here. Intrapopulation differences have been observed within Grand
560 Bank yellowtail flounder (Rideout and Morgan, 2007; Morgan and Rideout, 2008) as well as
561 other flatfish (Rijnsdorp, 1991; Kennedy et al., 2007), but not in all cases where it has been
562 examined (Nichol and Acuna, 2001; Kennedy et al., 2009). Spatial heterogeneity in condition
563 has been identified in yellowtail flounder on Georges Bank (Pereira et al., 2012); therefore based
564 on the present results it is expected that fecundity will covary among Georges Bank habitats with
565 condition. The Gulf of Maine and the southern New England/mid-Atlantic bight are not
566 completely homogeneous in environmental conditions, which could result in differing egg
567 production within these stock regions, especially given the high individual variability in PAF and
568 K_n observed for the samples here.
569
570 4.4 Magnitude and timing of down-regulation
571 Environmental factors that affect consumption, growth, and condition are likely
572 important for both understanding and prediction of PAF (Lambert et al., 2003; Wright, 2013).
573 Although PAF estimates covary with K_n, whether K_n determines PAF, or if they both are
574 affected by a common cause (e.g. seasonal energy intake) remains uncertain. Nevertheless, K_n at
575 the time of sampling, did account for some of the variation among years and stocks in fecundity

576 and levels of down-regulation. The highest down-regulation (as a percentage of PAF) in GOM
577 fish was observed in 2011, coincident with the lowest observed K_n. However these were not
578 always coincident; for example, K_n in 2011 for SNE fish was the highest observed, but down-
579 regulation was also high. High fecundity was only weakly correlated with condition, as
580 individual variation was substantial and condition also declined with increasing OD_{LC}. The
581 regression estimates of down-regulation among years did not completely mirror the direct
582 measures of atresia ($\%A_c$). Equivocal association between fecundity, K_n, and down-regulation is
583 partially attributable to the fact that the variables measured here (K_n, $\%A_c$, overall stock-wide
584 down-regulation) are point estimates of continuous processes and do not account for periods of
585 low condition or high down-regulation that may have occurred during other portions of the year.
586 Feeding and condition much earlier in the seasonal cycle, e.g. at the start of vitellogenesis, may
587 have greater impact on fecundity than condition just prior to spawning (Skjæraasen et al., 2006).
588 Likely a combination of condition, size at length (growth), and environmental factors throughout
589 the year contribute to PAF variation. Results here for yellowtail flounder indicate some
590 adjustment of fecundity during the months just prior to spawning, with fecundity down-
591 regulation related to very low relative condition during late vitellogenesis.
592 The timing of sampling can have consequences for fecundity estimation, and typically
593 researchers attempt to sample as close to, but prior to, spawning to avoid overestimating
594 fecundity (Murua et al., 2003; Ganias et al., 2014). The two thresholds related to oocyte diameter
595 measures employed here ensured that individuals had a distinct size hiatus in the distribution of
596 oocytes and that clutches were well developed. The yolked clutch exhibited variable size
597 distributions among individuals, and the use of a second threshold further excluded fish with
598 oocytes still in early development. Down-regulation of fecundity that occurred early in clutch

development was not accounted for applying these thresholds, and our estimates of down-regulation may underestimate total down-regulation of the clutch from initiation to maturation. Regardless, this approach assures our estimates of PAF are closer to the realized annual fecundity. Furthermore, inclusion of OD_{LC} in the final fecundity model accounted for down-regulation and individual variation in the stage of clutch development.

The stereological method applied in the current study is model based (requiring assumptions related to particle shape) and can introduce bias when attempting to obtain absolute counts, such as fecundity estimation, due to non-uniform shrinkage or distortion of the reference section (Kjesbu et al., 2010; Ganias et al., 2014). Unbiased methods (e.g. the dissector method) exist, but require multiple sequential histology sections which were not available. However, some of the assumptions and potential biases in the particle count approaches are avoided when relative intensities are estimated (Kjesbu et al. 2010), as was done here. Quantification and exclusion of negative sample area (empty space) from the calculations also reduced some of the bias related to distortion of sections. Another complication is that the size and shape of the cell types varies. We found the coefficients K and β differed among cell types, as also reported for bluefin tuna, *Thunnus thynnus* (Medina et al., 2002; Aragón et al., 2010), and used cell specific parameters derived herein (see methods) to account for shape differences. Although, some bias likely remains in this approach, the stereological estimates here provide useful relative measures of atresia levels for comparison to our whole mount fecundity and down-regulation analyses.

The two down-regulation approaches (the indirect fecundity model based and direct stereological estimates) provided independent measures to aid interpretation of the timing and processes involved in down-regulation. The image filtering employed in the fecundity processing excluded less-opaque and irregularly shaped atretic oocytes; thus many of the down-regulated

622 (atretic) oocytes were not included in fecundity estimates. The direct stereological approach
623 provides individual-level estimates of atresia, $\%A_c$ from 0-34% but typically <5%, that include
624 more atresia than that inferred from fecundity samples that likely excluded all β atresia and some
625 α-atretic oocytes. The low atresia rates reported here are consistent with those reported for
626 yellow tail flounder by Zamarro (1991) on the Grand Bank (<0.001%) and Howell (1983) in
627 SNE (0.4-1.8%). Howell (1983) used straight counts from histology, and the author
628 acknowledged this would underestimate the abundance of the smaller atretic oocytes relative to
629 the larger vitellogenic cells. Although general individual levels identified here were low for most
630 fish; some individual fish had high intensities of atresia.
631 The rate of degeneration of atretic oocytes relative to OD_{LC} is unknown for yellowtail
632 flounder, which precludes the simple expansion of atretic rates to estimate total atresia during the
633 entire development period of the annual cohort. Estimates for persistence of α atresia for other
634 species vary from 5-10 days (summarized by Witthames et al., 2010), although some α particles
635 persisted 150 days (though these were considered cysts). Though the duration β atretic particles
636 is uncertain, given the lower frequency observed (as compared to alpha) they are presumably less
637 persistent. Assuming similarly brief existence of atretic particles in yellowtail, any point
638 estimates represent a fraction of the total atresia during the period investigated. The point
639 estimates of atresia presented here potentially arise from different patterns of atresia. Individuals
640 probably also vary in their down-regulation pattern in response to certain internal or external
641 factors, which would contribute to the observed fecundity distribution. The theoretical patterns
642 for both the low steady and variable down-regulation patterns were parameterized using the
643 stereological estimates of atresia for yellowtail flounder and resulted in the PDF's closest to the
644 observed data. This suggests for the majority of fish there are low levels of atresia throughout the

645 late development of the clutch. However, a few fish were observed to have high rates of atresia.
646 If environmental or feeding conditions sufficient to cause substantial down-regulation do occur
647 at a regional scale, the mechanism for large-scale, stock-level decreases in egg production
648 appears to exist. In 2011, high down-regulation during the sampling period was observed in both
649 inshore stocks.

650 The estimated within stock atresia rates, roughly 3-25% reduction in PAF observed for
651 yellowtail flounder, were similar or below estimates for other species. Decreases in potential
652 fecundity of 45% have been reported for Greenland halibut, *Reinhardtius hippoglossoides*
653 (Kennedy et al., 2009), 27-30% in Atlantic cod, *Gadus morhua* (Witthames et al., 2013), and 20-
654 71% in Atlantic herring, *Clupea harengus* (Kurita et al., 2003; van Damme et al., 2009; Bucholtz
655 et al., 2013). Down-regulation may also occur at earlier stages of oogenesis than examined here;
656 as in some species where it has been found to be lower just prior to spawning and higher during
657 an earlier 'atretic' window (Kurita et al., 2003; Kennedy et al., 2009). Down-regulation of
658 yellowtail flounder was found to occur throughout late vitellogenesis. Additional but earlier
659 down-regulation may explain the weak relationship between predicted PAF residuals and $\%A_c$.
660 Many fish with negative PAF residuals did not exhibit high levels of atresia; therefore the lower
661 fecundity may be the result of some earlier down-regulation or of the initial clutch size. Howell
662 (1983) found vitellogenic atresia from November to May with the greatest intensities in January
663 and February, whereas none was observed June through October (a period of early
664 development). In the present study annual down-regulation rates and interannual variation in
665 PAF were not always correlated and this may indicate that final fecundity is a combination of
666 processes occurring both early and late in development. For this species, results herein and from
667 previous work suggest PAF can be adjusted over a broad oocyte development period, and there

668 may be plasticity in the seasonal timing and magnitude of fecundity regulation. The stock
669 differences also indicate the flexible nature of fecundity regulation, and that down-regulation and
670 final fecundity may be the result of local environmental and feeding conditions.
671
672 **5.0 Conclusions**
673 Yellowtail flounder fecundity was found to vary temporally and spatially, and was
674 inversely related to latitude. Stock-level fluctuations in condition and down-regulation suggest
675 environmental influences on development of the annual batch of eggs prior to spawning. Though
676 variable at both individual and stock levels, down-regulation was evident, underscoring the need
677 to account for the progression of clutch development in fecundity models. Fish size and relative
678 condition influence fecundity in this species, underscoring the importance of tracking temporal
679 and spatial growth variability in the stock assessment models. Future studies should explore
680 environmental drivers of size and condition to model variation in reproductive potential.
681 However, changes in egg production due to population size structure and relative condition alone
682 cannot fully explain the poor recruitment of yellowtail flounder in recent years. It is probable that
683 egg production in concert with other factors affecting egg, larval, and juvenile stages (e.g.
684 climate driven regulation of juvenile production; Sullivan et al., 2005), act synergistically to
685 contribute to recruitment variability.
686
687 **Acknowledgements**
688 We thank the organizers of the International Flatfish Symposium, editors of this symposium
689 special issue, and anonymous reviewers for their constructive suggestions. This study was
690 funded by the National Oceanic and Atmospheric Administration (NOAA), Northeast Fisheries

691 Science Center (NEFSC), Northeast Cooperative Research Program (NCRP). We thank NCRP's
692 Study Fleet staff and participating fishermen, Ecosystems Surveys Branch of the NOAA
693 Fisheries Northeast Fisheries Science Center and the officers and crew of the NOAA research
694 vessel H. B. Bigelow, and the Massachusetts Division of Marine Fisheries (MADMF) for
695 assistance securing biological samples utilized in this study. We thank all the staff members of
696 these various programs and in particular: J. Hoey (NEFSC-NCRP), J. Moser, M. Ball, and D. St.
697 Amand (NEFSC-Study Fleet), J. King (MADMF). Y. Press and J. Dayton assisted early
698 sampling and protocol development, and S. Emery aged all samples. L. O'Brien and C. Legault
699 provided valuable suggestions on an earlier version of the text and analyses. We also thank Mass
700 Histology Service Inc. for histological processing.

701

702 **References**

703

704 Alonso-Fernández, A., Vallejo, A.C., Saborido-Rey, F., Murua, H., Trippel, E.A., 2009.
705 Fecundity estimation of Atlantic cod (*Gadus morhua*) and haddock (*Melanogrammus aeglefinus*)
706 of Georges Bank: Application of the autodiametric method. Fish. Res. 99, 47-54.
707
708 Andersen, T.E., 2003. Unbiased stereological estimation of cell numbers and volume fractions:
709 the director and the principles of point counting, in: Kjesbu, O. S., Hunter, J. R., Witthames, P.
710 R. (Eds.), Report of the Working Group on Modern Approaches to Assess Maturity and
711 Fecundity of Warm- and Cold-water Fish and Squids. Havforskningsinstituttet, Bergen, Norway,
712 pp. 8-18.
713
714 Anderson, D.R., 2008. Model based inference in the life sciences: a primer on evidence. New
715 York, NY, Springer Science & Business Media LLC.
716
717 Aragón, L., Aranda, G., Santos, A., Medina, A, 2010. Quantification of ovarian follicles in
718 bluefin tuna *Thunnus thynnus* by two stereological methods. J. Fish Biol. 77, 719-730.
719
720 Benoît, H.P., Pepin, P., 1999. Interaction of rearing temperature and maternal influence on egg
721 development rates and larval size at hatch in yellowtail flounder (*Pleuronectes ferrugineus*). Can.
722 J. Fish. Aquat. Sci. 56, 785-794.
723
724 Blanchard, J.L., Frank, K.T., Simon, J.E., 2003. Effects of condition on fecundity and total egg
725 production of eastern Scotian Shelf haddock (*Melanogrammus aeglefinus*). Can. J. Fish. Aquat.

726 Sci. 60, 321-332.
727
728 Briggs, J.C., 1974. Marine Zoogeography. McGraw-Hill Book Co., New York.
729
730 Brooks, E.N., 2013. Effects of variable reproductive potential on reference points for fisheries
731 management. Fish. Res. 138, 152-158.
732
733 Bucholtz, R.H., Tomkiewicz, J., Nyengaard, J.R., Andersen, J.B., 2013. Oogenesis, fecundity
734 and condition of Baltic herring (*Clupea harengus* L.): A stereological study. Fish. Res. 145, 100-
735 113.
736
737 Buckley, L.J., Smigielski, A.S., Halavik, T.A., Caldarone, E.M., Burns, B.R., Laurence, G.C.,
738 1991. Winter flounder, *Pseudopleuronectes americanus*, reproductive success. II. Effects of
739 spawning time and female size on size, composition and viability of eggs and larvae. Mar. Ecol.
740 Prog. Ser. 74, 125-135.
741
742 Cadrin, S.X., 2010. Interdisciplinary analysis of yellowtail flounder stock structure off New
743 England. Rev. Fish. Sci. 18, 281-299.
744
745 Cooper, D.W., Maslenikov, K.P., Gunderson, D.R., 2007. Natural mortality rate, annual
746 fecundity, and maturity at length for Greenland halibut (*Reinhardtius hippoglossoides*) from the
747 northeastern Pacific Ocean. Fish. Bull. 105, 296-304.
748
749 DeCelles, G.R., Cadrin, S.X., 2011. An interdisciplinary assessment of winter flounder
750 (*Pseudopleuronectes americanus*) stock structure. J. Northw. Atl. Fish. Sci. 43, 103-120.
751
752 Emerson, L.S., Greer Walker, M., Witthames, P.R., 1990. A stereological method for estimating
753 fish fecundity. J. Fish Biol. 36, 721-730.
754
755 Fitzhugh, G.R., Shertzer, K.W., Kellison, G.T., Wyanski, D.M., 2012. Review of size- and age-
756 dependence in batch spawning: implications for stock assessment of fish species exhibiting
757 indeterminate fecundity. Fish. Bull. 110, 413–425.
758
759 Ganias K., Murua H., Claramunt G., Dominguez-Petit R., Gonçalves P., Juanes F., Keneddy J.,
760 Klibansky N., Korta M., Kurita Y., Lowerre-Barbieri S., Macchi G., Matsuyama M., Medina A.,
761 Nunes C., Plaza G., Rideout R., Somarakis S., Thorsen A., Uriarte A., Yoneda M. 2014. Chapter
762 4: Egg production, 109 pp. *In Handbook of applied fisheries reproductive biology for stock*
763 *assessment and management, ed.* R. Domínguez-Petit, H. Murua, F. Saborido-Rey and E.
764 Trippel. Vigo, Spain. Digital CSIC. http://hdl.handle.net/10261/87768.
765
766 Horwood, J.W., Walker, M.G., Witthames, P., 1989. The effect of feeding levels on the
767 fecundity of plaice (*Pleuronectes platessa*). J. Mar. Biol. Assoc. U. K. 69, 81-92.
768
769 Howell, W.H., 1983. Seasonal changes in the ovaries of adult yellowtail flounder, *Limanda*
770 *ferruginea*. Fish. Bull. 81, 341-355.
771

772 Howell, W.H., Kesler, D.H., 1977. Fecundity of the southern New England stock of yellowtail
773 flounder, *Limanda ferruginea*. Fish. Bull. 75, 877-880.
774
775 Hunter, J.R., Macewicz, B.J., 1985. Rates of atresia in the ovary of captive and wild northern
776 anchovy, *Engraulis mordax*. Fish. Bull. 83, 119-136.
777
778 Kennedy, J., Geffen, A.J., Nash, R.D.M., 2007. Maternal influences on egg and larval
779 characteristics of plaice (*Pleuronectes platessa* L.). J. Sea Res. 58, 65-77.
780
781 Kennedy, J., Gundersen, A.C., Boje, J., 2009. When to count your eggs: Is fecundity in
782 Greenland halibut (*Reinhardtius hippoglossoides* W.) down-regulated? Fish. Res. 100, 260-265.
783
784 Kjesbu, O.S., Fonn, M., Gonzáles, B.D., Nilsen, T., 2010. Stereological calibration of the profile
785 method to quickly estimate atresia levels in fish. Fish. Res. 104, 8-18.
786
787 Kjesbu, O.S., Solemdal, P., Bratland, P., Fonn, M., 1996. Variation in annual egg production in
788 individual captive Atlantic cod (*Gadus morhua*). Can. J. Fish. Aquat. Sci. 53, 610-620.
789
790 Kjesbu, O.S., Witthames, P.R., 2007. Evolutionary pressure on reproductive strategies in flatfish
791 and groundfish: Relevant concepts and methodological advancements. J. Sea Res. 58, 23-34.
792
793 Kurita, Y., Meier, S., Kjesbu, O.S., 2003. Oocyte growth and fecundity regulation by atresia of
794 Atlantic herring (*Clupea harengus*) in relation to body condition throughout the maturation
795 cycle. J. Sea Res. 49, 203-219.
796
797 Lambert, Y., 2013. Long-term changes in life history characteristics and reproductive potential
798 of northern Gulf of St. Lawrence cod (*Gadus morhua*) and consequences for the stock
799 productivity. Fish. Res. 138, 5-13.
800
801 Lambert, Y., Yaragina, N.A., Kraus, G., Marteinsdóttir, G., Wright, P.J., 2003. Using
802 environmental and biological indices as proxies for egg and larval production of marine fish. J.
803 Northw. Atl. Fish. Sci. 33, 115-159.
804
805 Le Cren, E.D., 1951. The length-weight relationship and seasonal cycle in gonad weight and
806 condition in the perch (*Perca fluviatilis*). J. Anim. Ecol. 20, 201-219.
807
808 Legault, C.M., Alade, L., Gross, W.E., and Stone, H.H. 2013. Stock Assessment of Georges
809 Bank Yellowtail Flounder for 2013. TRAC (Transboundary Resources Assessment Committee)
810 Ref. Doc. 2013/01. http://www.bio.gc.ca/info/intercol/trac-cert/publications-eng.php.
811
812 Lowerre-Barbieri, S.K., Brown-Peterson, N.J., Murua, H., Tomkiewicz, J., Wyanski, D.M.,
813 Saborido-Rey, F., 2011. Emerging issues and methodological advances in fisheries
814 reproductive biology. Mar. Coast. Fish. 3, 32-51.
815
816 Manning, A.J. Crim, L.W., 1998. Maternal and interannual comparison of the ovulatory
817 periodicity, egg production and egg quality of the batch-spawning yellowtail flounder. J. Fish

818 Biol. 53, 954-972.
819
820 Marshall, C.T., O'Brien, L., Tomkiewicz, J., Koster, F.W., Kraus, G., Marteinsdottir, G., et al.,
821 2003. Developing alternative indices of reproductive potential for use in fisheries management:
822 case studies for stocks spanning an information gradient. J. Northwest Atl. Fish. Sci. 33, 161-
823 190.
824
825 Marteinsdottir, G., Thorarinsson, K., 1998. Improving the stock-recruitment relationship in
826 Icelandic cod (*Gadus morhua* L.) by including age diversity of spawners. Can. J. Fish. Aquat.
827 Sci. 55, 1372-1377.
828
829 McElroy, W.D., Wuenschel, M.J., Press, Y.K., Towle, E.K., McBride, R.S., 2013. Differences in
830 female individual reproductive potential among three stocks of winter flounder,
831 *Pseudopleuronectes americanus*. J. Sea Res. 75, 52-61.
832
833 Medina, A., Abascal, F.J., Megina, C., García, A., 2002. Stereological assessment of the
834 reproductive status of female Atlantic northern bluefin tuna during migration to Mediterranean
835 spawning grounds through the Strait of Gibraltar. J. Fish Biol. 60, 203-217.
836
837 Morgan, M.J., 2008. Integrating reproductive biology into scientific advice for fisheries
838 management. J. Northwest Atl. Fish. Sci. 41, 37-51.
839
840 Morgan, J.M., Murua, H., Kraus, G., Lambert, Y., Marteinsdótter, G., Marshall, C.T., O'Brien,
841 L., Tomkiewicz, J., 2009. The evaluation of reference points and stock productivity in the
842 context of alternative indices of stock reproductive potential. Can. J. Fish. Aquat. Sci. 66, 404-
843 414.
844
845 Morgan, M.J., Perez-Rodriguez, A., Saborido-Rey, F., 2011. Does increased information about
846 reproductive potential result in better prediction of recruitment? Can. J. Fish. Aquat. Sci. 68,
847 1361–1368.
848
849 Morgan, M.J., Rideout, R.M., 2008. The impact of intrapopulation variability in reproductive
850 traits on population reproductive potential of Grand Bank American plaice (*Hippoglossoides*
851 *platessoides*) and yellowtail flounder (*Limanda ferruginea*). J. Sea Res. 59, 186-197.
852
853 Morgan, M.J., Rideout, R.M., Colbourne, E.B., 2010. Impact of environmental temperature on
854 Atlantic cod, *Gadus morhua*, energy allocation to growth, condition and reproduction. Mar. Ecol.
855 Prog. Ser. 404, 185-195.
856
857 Murua, H., Kraus, G., Saborido-Rey, F., Witthames, P., Thorsen, A., Junquera, S., 2003.
858 Procedures to estimate fecundity of marine fish species in relation to their reproductive strategy.
859 J. Northwest Atl. Fish. Sci. 33, 33-54.
860
861 NEFSC (Northeast Fisheries Science Center), 2012a. 54th Northeast Regional Stock Assessment
862 Workshop (54th SAW) Assessment Report. US Dept. Commer., Northeast Fish. Sci. Cent. Ref.
863 Doc. 12-18

NEFSC (Northeast Fisheries Science Center), 2012b. Assessment or Data Updates of 13 Northeast Groundfish Stocks through 2010. US Dept. Commer., Northeast Fish. Sci. Cent. Ref. Doc. 12-06.

Nichol, D.G., Acuna, E.I., 2001. Annual and batch fecundities of yellowfin sole, *Limanda aspera*, in the eastern Bering Sea. Fish. Bull. 99, 108-122.

Penttila, J., Dery, L.M. (Eds.), 1988. Age determination methods for Northwest Atlantic species. NOAA Tech. Rep. NOAA-TR-NMFS-72, Northeast Fisheries Science Center, Woods Hole, MA (USA).

Pereira, J., Schultz, E.T., Auster, P.J., 2012. Geospatial analysis of habitat use in yellowtail flounder *Limanda ferruginea* on Georges Bank. Mar. Ecol. Prog. Ser. 468, 279-290.

Pitt, T.K., 1971. Fecundity of the yellowtail flounder (*Limanda ferruginea*) from the Grand Bank, Newfoundland. J. Fish. Res. Board Can. 28, 456-457.

R Development Core Team, 2013. R: A Language and Environment for Statistical Computing. R Foundation for Statistical Computing, Vienna, Austria.

Rideout, R.M., Morgan, M.J., 2007. Major changes in fecundity and the effect on population egg production for three species of north-west Atlantic flatfishes. J. Fish Biol. 70, 1759-1779.

Rideout, R.M., Morgan, M.J., 2010. Relationships between maternal body size, condition and potential fecundity of four north-west Atlantic demersal fishes. J. Fish Biol. 76, 1379-1395.

Rijnsdorp, A. D., 1991. Changes in fecundity of female North Sea plaice (*Pleuronectes platessa* L.) between three periods since 1900. ICES J. Mar. Sci. 48, 253-280.

Saborido-Rey, F., Trippel, E.A., 2013. Fish reproduction and fisheries. Fish. Res. 138, 1-4.

Skjæraasen, J. E., Nilsen, T., Kjesbu, O.S., 2006. Timing and determination of potential fecundity in Atlantic cod (*Gadus morhua*). Can. J. Fish. Aquat. Sci. 63, 310-320.

Stares, J.C., Rideout, R.M., Morgan, M.J., Brattey, J., 2007. Did population collapse influence individual fecundity of northwest Atlantic cod? ICES J. Mar. Sci. 64, 1338-1347.

Sterio, D.C., 1984. The unbiased estimation of number and sizes of arbitrary particles using the disector. J. Microsc. 134, 127-136.

Sullivan, M.C., Cowen, R.K., Steves, B.P., 2005. Evidence for atmosphere-ocean forcing of yellowtail flounder (*Limanda ferruginea*) recruitment in the Middle Atlantic Bight. Fish. Oceanogr. 14, 386-399.

Thorsen, A., Kjesbu, O.S., 2001. A rapid method for estimation of oocyte size and potential

910 fecundity in Atlantic cod using a computer-aided particle analysis system. J. Sea Res. 46, 295-
911 308.
912
913 Thorsen, A., Witthames, P.R., Marteinsdóttir, G., Nash, R.D.M., Kjesbu, O.S., 2010. Fecundity
914 and growth of Atlantic cod (*Gadus morhua* L.) along a latitudinal gradient. Fish. Res. 104, 45-
915 55.
916
917 Tomkiewicz, J., Morgan, M.J., Burnett, J., Saborido-Rey, F., 2003. Available information for
918 estimating reproductive potential of northwest Atlantic groundfish stocks. J. Northwest Atl. Fish.
919 Sci. 33, 1-21.
920
921 Trippel, E.A., 1999. Estimation of stock reproductive potential: History and challenges for
922 Canadian Atlantic gadoid stock assessments. J. Northwest Atl. Fish. Sci. 25, 61-81.
923
924 Trippel, E.A., Neil, S.R.E., 2004. Maternal and seasonal differences in egg sizes and spawning
925 activity of northwest Atlantic haddock (*Melanogrammus aeglefinus*) in relation to body size and
926 condition. Can. J. Fish. Aquat. Sci. 61, 2097–2110.
927
928 van Damme, C.J.G., Dickey-Collas, M., Rijnsdorp, A.D., Kjesbu, O.S., 2009. Fecundity, atresia,
929 and spawning strategies of Atlantic herring (*Clupea harengus*). Can. J. Fish. Aquat. Sci. 66,
930 2130-2141.
931
932 Weibel, E.R., 1979. Stereological methods. Vol. 1. Practical methods for biological
933 morphometry. Academic Press, London.
934
935 Weibel, E.R., Gomez, D.M., 1962. A principle for counting tissue structures on random sections.
936 J. Appl. Physiol. 17, 343-348.
937
938 Weibel, E.R., Kistler, G.S., Scherle, W.F., 1966. Practical stereological methods for
939 morphometric cytology. J. Cell Biol. 30, 23-38.
940
941 Wirgin, I., Maceda, L., Grunwald, C., Roy, N.K., Waldman, J.R., 2014. Coastwide stock
942 structure of winter flounder using nuclear DNA analyses. Trans. Am. Fish. Soc. 143, 240-251.
943
944 Witthames, P.R., Armstrong, M., Thorsen, A., Solemdal, P., Kjesbu, O.S., 2013. Contrasting
945 development and delivery of realised fecundity in Atlantic cod (*Gadus morhua*) stocks from cold
946 and warm waters. Fish. Res. 138, 128-138.
947
948 Witthames, P.R., Greenwood, L.N., Thorsen, A., Dominguez, R., Murua, H., Korta, M.,
949 Saborido-Rey, F., Kjesbu, O.S., 2009. Advances in methods for determining fecundity:
950 application of the new methods to some marine fishes. Fish. Bull. 107, 148–164.
951
952 Witthames, P.R., Greer Walker, M., 1995. Determination of fecundity and oocyte atresia in sole
953 (*Solea solea*) (Pisces) from the Channel, the North Sea and the Irish Sea. Aquat. Living
954 Resour. 8, 91-109.
955

Witthames, P.R., Thorsen, A., Kjesbu, O.S., 2010. The fate of vitellogenic follicles in experimentally monitored Atlantic cod *Gadus Morhua* (L.): Application to stock assessment. Fish. Res. 104, 27-37.

Wootton, R.J., 1990. Ecology of Teleost Fishes. Chapman & Hall, London.

Wright, P.J., 2013. Methodological challenges to examining the causes of variation in stock reproductive potential. Fish. Res. 138, 14-22.

Zamarro, J., 1991. Batch fecundity and spawning frequency of yellowtail flounder (*Limanda ferruginea*) on the Grand Bank. Northwest Atl. Fish. Organ. Sci. Counc. Stud. 15, 43-51.

968 Table 1. Summary statistics for yellowtail flounder used to estimate potential annual fecundity
969 by stock area (Gulf of Maine [GOM], Georges Bank [GB], Southern New England [SNE]) and
970 spawning[a] year (means listed with ranges in parentheses).

		GOM	GB	SNE
n	2010	62	14	59
	2011	64	18	48
	2012	88	18	39
	Total	214	50	146
Total Length (mm)	2010	381 (280 - 550)	385 (352 - 423)	395 (284 - 465)
	2011	362 (313 - 459)	390 (340 - 430)	398 (315 - 465)
	2012	362 (295 - 450)	389 (300 - 465)	374 (295 - 464)
Fish Age (yr)	2010	4.2 (3 – 9)	4.0 (3 – 5)	4.4 (2 – 6)
	2011	3.6 (2 – 6)	4.2 (3 – 6)	4.6 (3 – 7)
	2012	4.2 (3 – 7)	4.4 (3 – 7)	4.2 (2 – 8)

971
972 [a] One fish each from SNE and GOM were captured in December 2010 and combined with 2011
973 samples – the year they would have spawned.
974

Table 2. Models predicting potential annual fecundity were compared for single predictor (a) or multiple predictors (b) using natural log-transformed total length (TL). Additional terms included stock (ST), year (YR), relative condition (K_n), and mean oocyte diameter of the leading cohort (OD_{LC}), and a stock-year interaction term (ST:YR). All potential model combinations for these parameters were tested, but only the best model for each number of terms is shown; where the best models were not distinguishable multiple models are shown for that number of terms. Models were evaluated based on the number of estimable parameters (K), log-likelihood (LL), the second order Akaike's Information Criterion (AICc), change in the AICc (ΔAICc), the AICc weight (wt.), and coefficient of determination (r^2). Model analysis was conducted on overlapping length ranges for SNE and GOM stocks across years rounded to the nearest cm (33 – 46 cm TL [n = 338]).

a	K	LL	AICc	Δ AICc	AIC wt.	r^2
TL	3	-42.9	91.9	--	0.000	0.62
ST	3	-145.6	297.2	205.3	0.000	0.30
YR	3	-172.4	352.9	261.0	0.000	0.17
K_n	3	-189.4	384.8	292.9	0.000	0.09
OD_{LC}	3	-204.4	414.8	322.9	0.000	< 0.01

b	K	LL	AICc	Δ AICc	AIC wt.	r^2
TL + ST + K_n + OD_{LC} + YR + ST:YR	8	70.9	-121.2	--	0.999	0.80
TL + ST + K_n + OD_{LC} + YR	7	61.9	-107.4	13.7	0.001	0.79
TL + ST + K_n + OD_{LC}	6	48.6	-85.0	36.1	0.000	0.78
TL + ST + K_n + YR	6	49.2	-84.0	37.2	0.000	0.78
TL + ST + K_n	6	31.6	-53.0	68.1	0.000	0.75
TL + K_n	5	3.8	0.5	121.7	0.000	0.71
TL	3	-42.9	91.9	213.1	0.000	0.62

Table 3. Regression coefficients for natural log-transformed linear regressions of potential annual fecundity of yellowtail flounder from each stock (by year and all years combined) are relative to either total length (TL) or fish age (FA) with standard errors (in parentheses for the intercept, α and the slopes: β_1 - β_3). Terms for the mean oocyte diameter of the leading cohort (OD_{LC}) and relative condition (K_n) are included. Isometric slopes, $\beta_1 = 3$ for TL and $\beta_1 = 1$ for FA, were evaluated using Wald *t*-tests. Regressions were determined over full range of FA or TL except rare lengths (TL < 300 mm or TL > 500 mm) and ages (FA = 2) were excluded ($n = 10$).

TL	Stock	Year	α	β_1 (TL)	β_2 (OD_{LC})	β_3 (K_n)	r^2	n	TL range	t ($\beta_1 = 3$)	p ($\beta_1 = 3$)
	GOM	2010	-9.0417 (2.3966)	3.7931 (0.4102)	-0.0008 (0.0007)	1.2065 (0.4297)	0.64	59	323 - 450	1.93	0.06
		2011	-6.6493 (2.2697)	3.5552 (0.3944)	-0.0029 (0.0008)	0.9617 (0.4499)	0.59	62	313 - 459	1.41	0.16
		2012	-4.5270 (1.8744)	3.0640 (0.3141)	-0.0012 (0.0005)	0.9658 (0.2265)	0.54	87	325 - 450	0.20	0.84
		All	-9.2454 (1.2558)	3.9049 (0.2128)	-0.0021 (0.0004)	1.2005 (0.2010)	0.64	208	313 - 459	4.25	*< 0.01*
	GB	All	-6.1022 (4.3530)	3.0610 (0.7013)	-0.0008 (0.0010)	2.3516 (0.5045)	0.42	50	300 - 465	0.09	0.93
	SNE	2010	-8.2958 (2.1794)	3.6184 (0.3434)	-0.0003 (0.0006)	1.3492 (0.3957)	0.69	57	337 - 465	1.80	0.08
		2011	-6.4841 (1.8246)	3.5334 (0.2999)	-0.0014 (0.0007)	0.5998 (0.2582)	0.76	48	315 - 465	1.78	0.08
		2012	-8.6858 (1.8052)	3.7297 (0.2776)	-0.0012 (0.0006)	1.4245 (0.3570)	0.86	37	327 - 464	2.64	*0.01*
		All	-8.2747 (1.1116)	3.7262 (0.1754)	-0.0011 (0.0004)	1.0475 (0.1891)	0.77	142	315 - 465	4.14	*< 0.01*

FA	Stock	Year	α	β_1 (FA)	β_2 (OD_{LC})	β_3 (K_n)	r^2	n	FA range	t ($\beta_1 = 1$)	p ($\beta_1 = 1$)
	GOM	2010	12.5035 (0.8814)	0.3986 (0.2548)	0.0003 (0.0012)	1.1646 (0.6802)	0.11	59	3 - 6	-2.36	*0.02*
		2011	12.5715 (0.9602)	0.4022 (0.2341)	-0.0003 (0.0011)	1.0262 (0.6906)	0.07	60	3 - 6	-2.55	*0.01*
		2012	13.0032 (0.5106)	0.2823 (0.1260)	-0.0001 (0.0007)	0.5587 (0.3414)	0.08	81	3 - 7	-5.70	*< 0.01*
		All	12.8163 (0.4479)	0.4232 (0.1180)	-0.0009 (0.0006)	1.0692 (0.3255)	0.11	200	3 - 7	-4.89	*< 0.01*
	GB	All	11.5782 (0.7591)	0.8187 (0.2386)	-0.0010 (0.0011)	1.8150 (0.5248)	0.35	49	3 - 7	-0.76	0.45
	SNE	2010	12.8173 (0.6341)	0.8780 (0.1054)	0.0002 (0.0007)	0.4230 (0.4885)	0.59	55	3 - 6	-1.16	0.25
		2011	13.7954 (0.6860)	0.8610 (0.1476)	-0.0014 (0.0011)	0.2173 (0.3890)	0.44	48	3 - 7	-0.94	0.35
		2012	12.0734 (0.9117)	0.9640 (0.1303)	-0.0016 (0.0010)	1.6122 (0.5857)	0.65	36	3 - 8	-0.28	0.78
		All	13.0707 (0.4396)	0.9039 (0.0772)	-0.0012 (0.0005)	0.7013 (0.2798)	0.52	139	3 - 8	-1.24	0.22

Table 4. Estimated cumulative down-regulation of yellowtail flounder fecundity as the mean oocyte diameter for the leading cohort increased from 400 to 500 μm. Predicted PAF (pPAF, in millions) at each mean oocyte diameter of the leading cohort ($pPAF_{400}$ and $pPAF_{500}$) was calculated for a typical total length (400 mm TL) using the regressions for each stock (ST) and year (YR) with the term for relative condition set a 1.0 ('average condition').

ST	YR	$pPAF_{400}$	$pPAF_{500}$	% Change
GOM	2010	2.13	1.96	-7.69
	2011	1.92	1.45	-24.86
	2012	1.62	1.43	-11.68
GB	All	1.55	1.42	-8.06
SNE	2010	2.21	2.14	-3.10
	2011	2.53	2.21	-12.70
	2012	2.22	1.97	-11.15

Table 5. Summary of potential annual fecundity estimates for yellowtail flounder at two common lengths (370 and 420 mm TL) covered by all studies. Fecundity calculated from previous studies using reported regressions for each location. . Estimates for the current study were calculated using mean oocyte diameter of the leading cohort = 500 μm and a relative condition = 1.0 ('average condition') for each stock and year independently, except all years combined for GB.

				Fecundity (millions)	
Study	Location	Sampling year (s)	*n*	370 mm	420 mm
Pitt (1971)	Grand Bank	1966 - 1967	51	0.80	1.46
Rideout & Morgan (2007)	Grand Bank (3LNO)	1993 - 1998	444	0.73	1.06
	Grand Bank (3Ps)	1993 - 1998	102	0.92	1.36
Howell & Kesler (1977)	SNE	1976	64	1.11	1.80
Current Study	GOM	2010	59	1.46	2.36
	GOM	2011	62	1.10	1.72
	GOM	2012	87	1.13	1.66
	GB	2010 - 2012	50	1.12	1.65
	SNE	2010	57	1.61	2.55
	SNE	2011	48	1.68	2.62
	SNE	2012	37	1.47	2.36

Fig. 1. Capture locations of yellowtail flounder sampled for fecundity during 2010-2012 (n = 410). Solid lines indicate boundaries for the three stocks: Gulf of Maine (GOM), Georges Bank (GB), and Southern New England (SNE). Box on inset map indicates the location of the study region off the U.S. Atlantic coast.

Fig. 2. Photomicrographs of two pre-spawning yellowtail flounder ovaries showing late vitellogenic (LV) and alpha (α) or beta (β) atretic oocytes. Images are overlaid with a Weibel dissector grid showing sampling points at both ends of each thin black line where the structure type was recorded. To ensure the count of each cell type is unbiased, oocytes transecting the top and right (grey) 'allowed' borders (e.g. oocyte A) are counted, and cells transecting the left and bottom (black) 'forbidden' borders (e.g. oocyte B) are not counted. Scale bar in bottom left is 250 μm.

Fig. 3. Yellowtail flounder potential annual fecundity (PAF) relative to total length (TL, left column) and fish age (FA, right column) by year and stock (on a log-log scale). GB regression is for all years combined. Lines are predicted PAF at length or age with terms for mean oocyte diameter of the leading cohort = 500 μm and relative condition = 1.0 ('average condition'). Ages jittered to reduce over-plotting. Rare lengths (TL < 300 mm or TL > 500 mm) and ages (FA = 2) were excluded from regression calculations (circled, n = 10).

Fig. 4. Potential annual fecundity (PAF) model estimates at age (a) and length (b) for yellowtail flounder sampled in each year from the SNE and GOM stocks. Estimates were calculated from linear regressions determined over a range of total lengths (rounded to nearest cm, 33 – 45 cm, n = 338) sampled from both stocks in all years (both age and length are on a log scale). All PAF models shown were calculated with mean oocyte diameter of the leading cohort = 500 μm and for relative condition = 1.0 ('average condition'). Predicted length at age (c) was plotted for each stock-year combination as determined from the same data subset using least-squares fit linear regression.

Fig. 5. Relative condition (K_n) of female yellowtail flounder by stock and year. Differences were evaluated across all but GB which were not included because of low sample size but are shown for comparison. Groups with matching letters were not significantly different from each other (p > 0.05; Tukey HSD post-hoc test).

Fig. 6. Length-predicted potential annual fecundity (PAF) residuals relative to condition (a, K_n) and mean oocyte diameter of the leading cohort (b, OD_{LC}). Predicted PAF values were determined using year-stock specific regressions for GOM and SNE females and for all years combined for GB females. The regressions used for predicting PAF in panel a included a term for OD_{LC} (but no K_n term) and those in panel b included a term for K_n (but no OD_{LC} term). Dashed lines are the least-squares fit linear regressions.

Fig. 7. The relative intensity of combined (α and β) atresia ($\%A_c$) estimated using stereology relative to mean whole-mount oocyte diameter of the leading cohort (a, OD_{LC}, n = 164). The solid line is the least-squares fit of the linear regression for $\%A_c$, and regressions for α ($\%A_\alpha$) and β ($\%A_\beta$) atresia were also plotted independently (points not shown). Relationship of $\%A_c$ relative

1063 to condition (b, K_n) with a reference line (solid) indicating 'average' condition, and the dashed
1064 line the least-squares fit of the linear regression.
1065
1066 Fig. 8. Stereological estimates of the relative intensity of combined (α and β, $\%A_c$) atresia by
1067 stock and year. Sample size was 20 fish for each year in GOM and SNE stocks, but for GB were
1068 n = 9, 17, and 18 fish in 2010 - 2012, respectively.
1069
1070 Fig. 9. Left column, declines in relative fecundity as the annual clutch of oocytes develops
1071 (relative to the mean oocyte diameter of the leading cohort, OD_{LC}) for different theoretical
1072 patterns of atretic down-regulation. Right column, kernal density functions for the predicted
1073 relative fecundity under each modeled atresia rate (scaled to the frequency of observed
1074 diameters) and the observed frequency for yellowtail flounder fecundity.

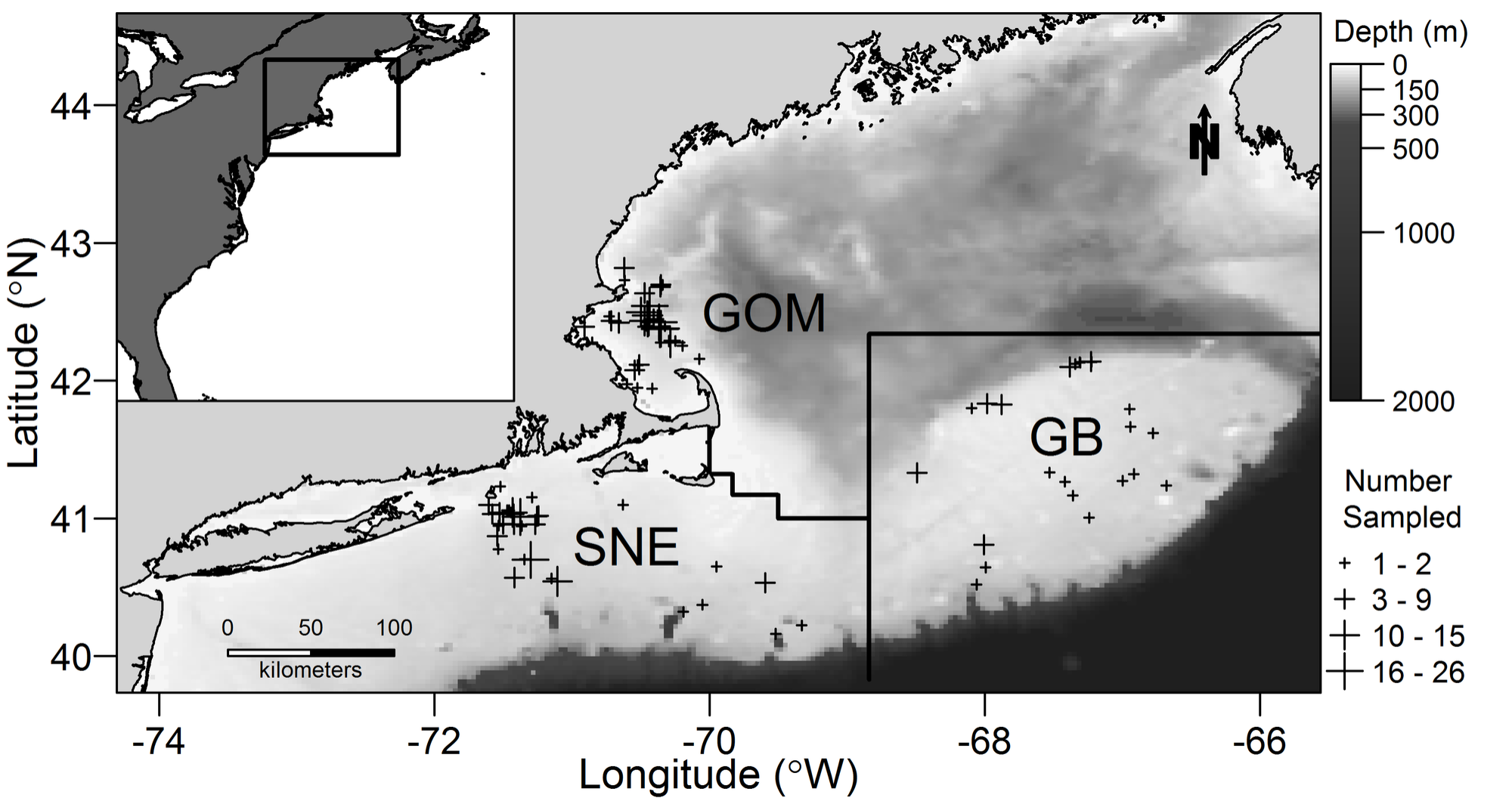
Depth (m)
0
150
300
500
1000
2000
GOM
GB
SNE
N
Number Sampled
1 - 2
3 - 9
10 - 15
16 - 26
0
50
100
kilometers
Latitude (°N)
44
43
42
41
40
-74
-72
-70
-68
-66
Longitude (°W)

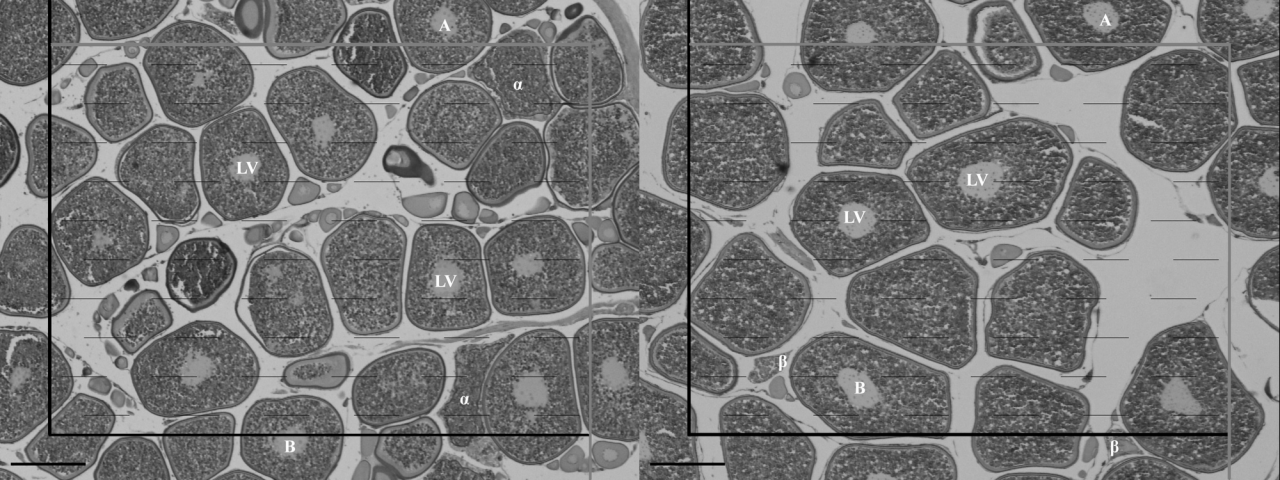
A
α
LV
LV
α
B
A
LV
LV
β
B
β

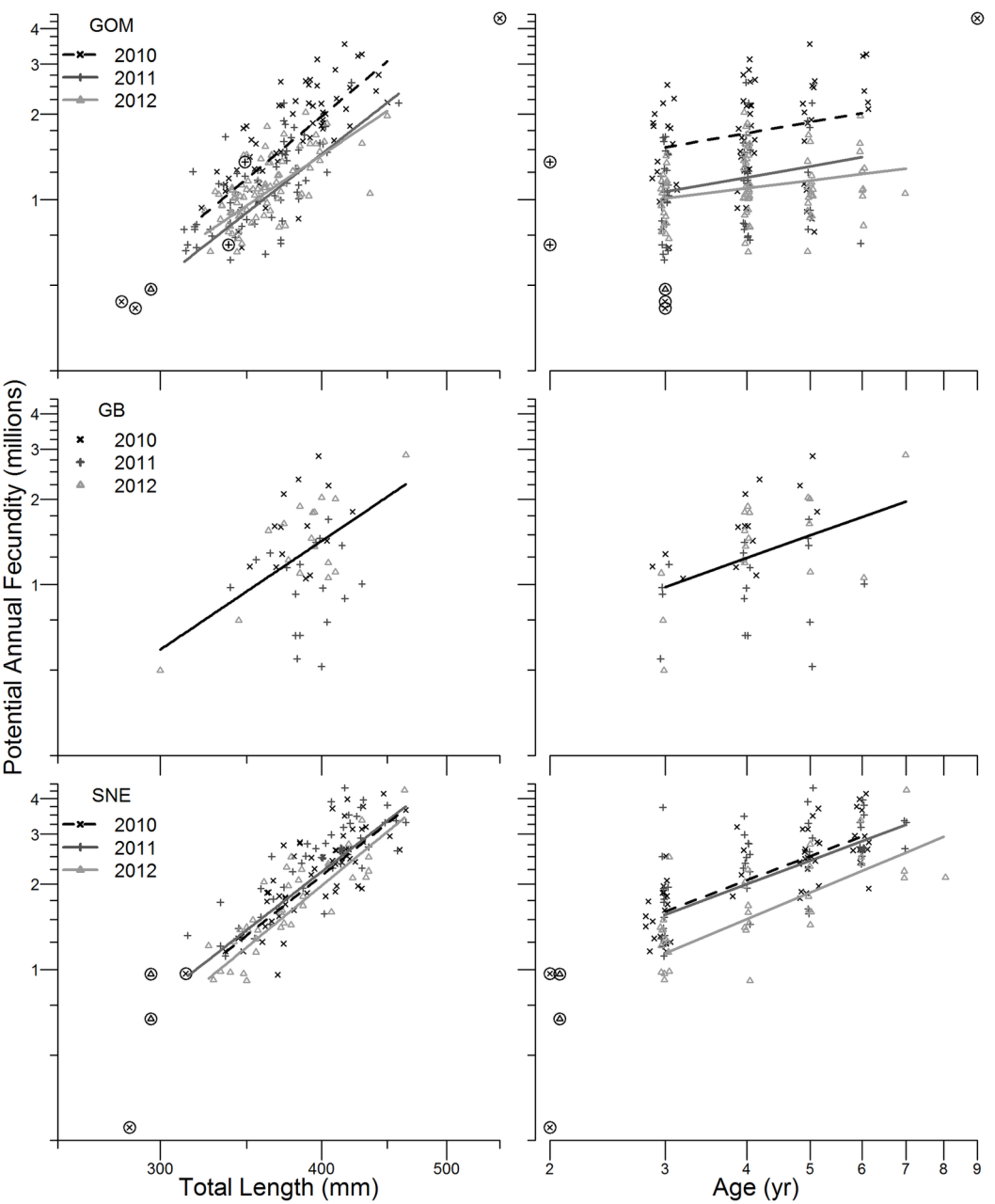
GOM
2010
2011
2012
GB
2010
2011
2012
SNE
2010
2011
2012
Potential Annual Fecundity (millions)
Total Length (mm)
Age (yr)

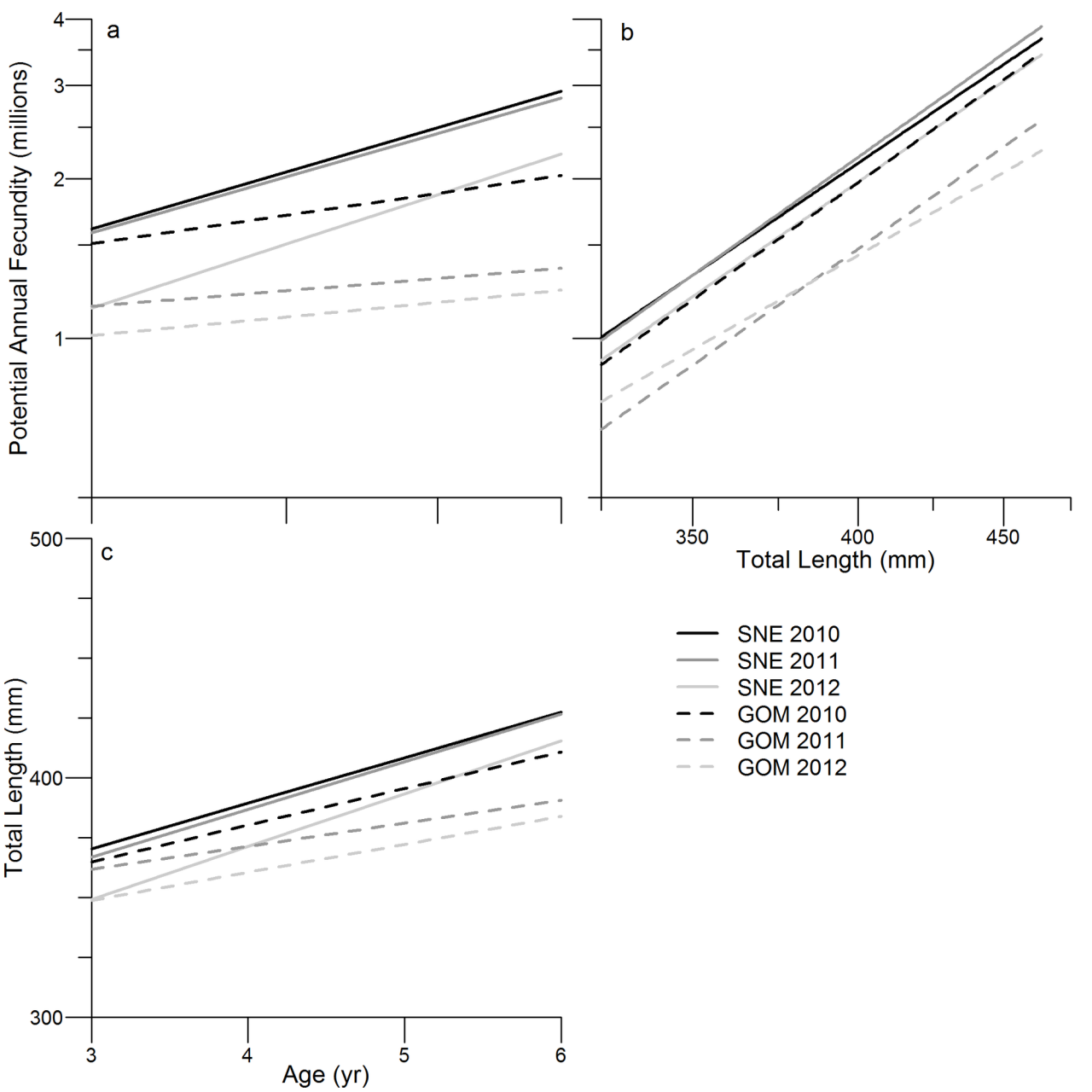
a
b
c
Potential Annual Fecundity (millions)
Total Length (mm)
Age (yr)
SNE 2010
SNE 2011
SNE 2012
GOM 2010
GOM 2011
GOM 2012

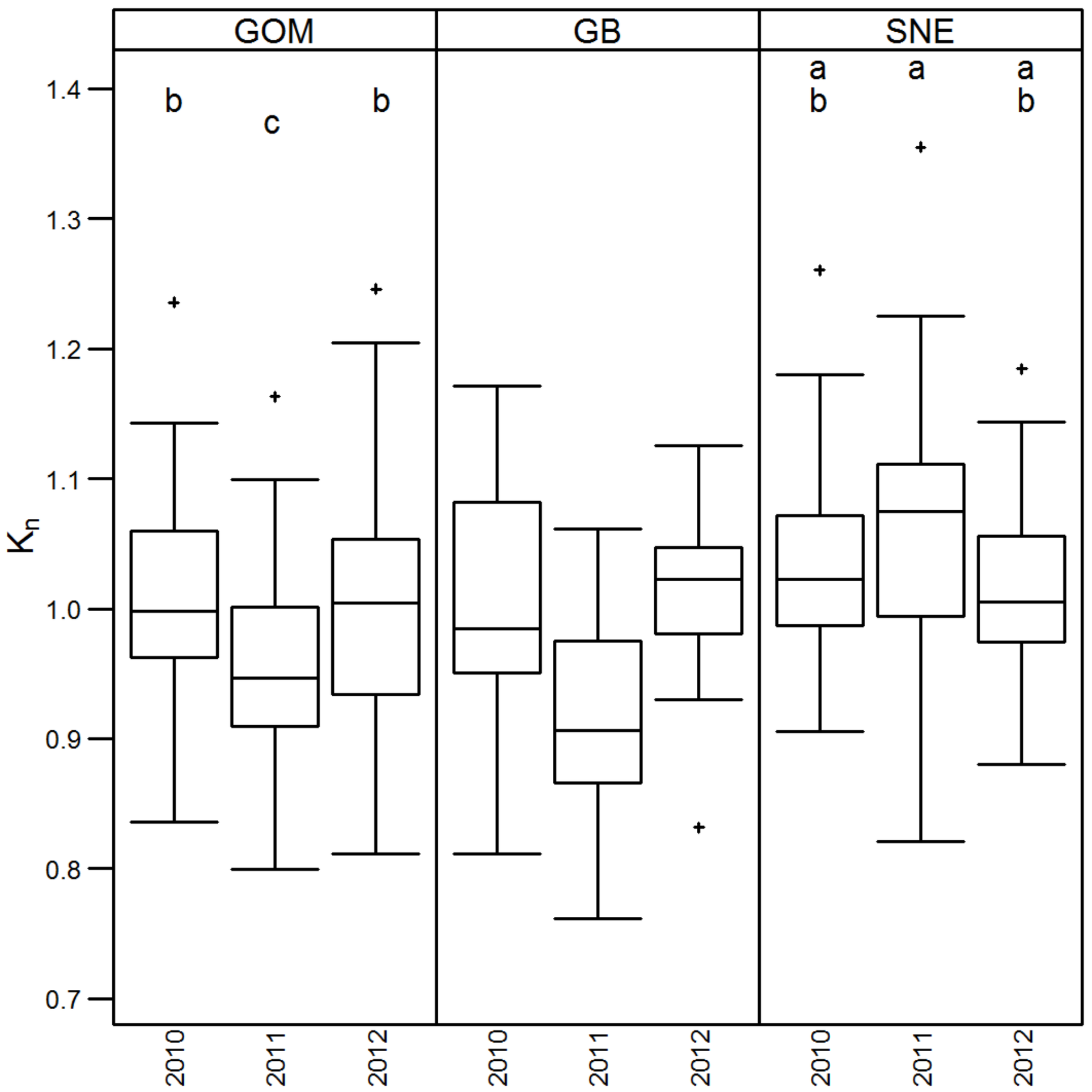
GOM
GB
SNE
K_n
1.4
1.3
1.2
1.1
1.0
0.9
0.8
0.7
b
c
b
a
b
a
a
b
2010
2011
2012
2010
2011
2012
2010
2011
2012

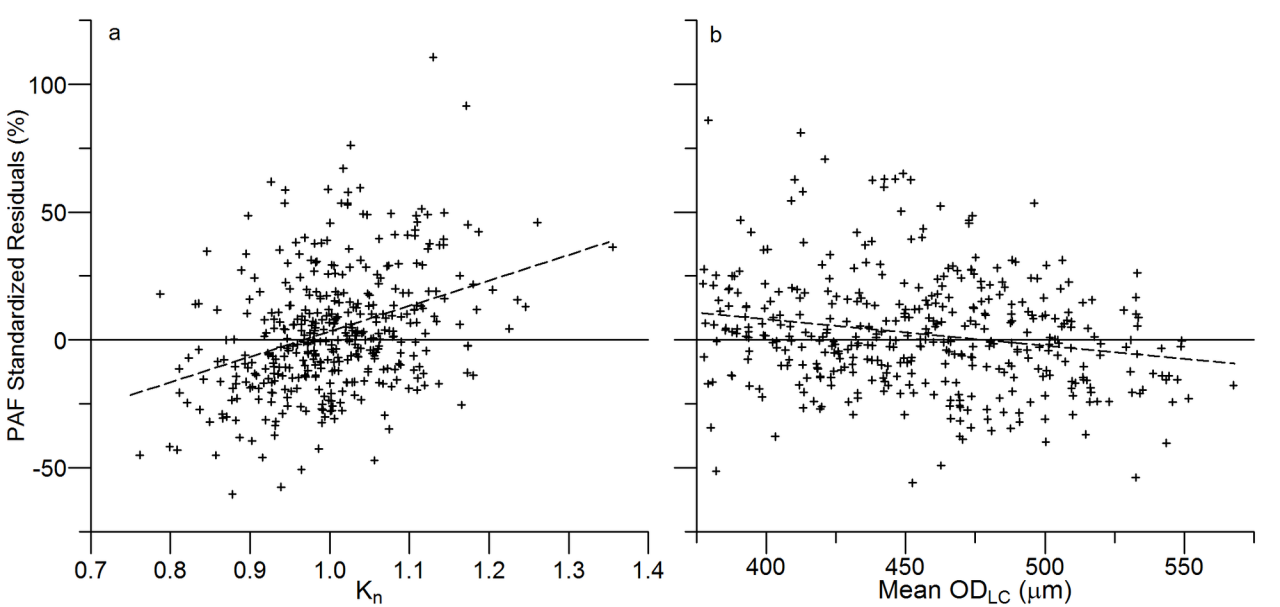
a
b
PAF Standardized Residuals (%)
100
50
0
-50
0.7
0.8
0.9
1.0
1.1
1.2
1.3
1.4
K_n
400
450
500
550
Mean OD_{LC} (μm)

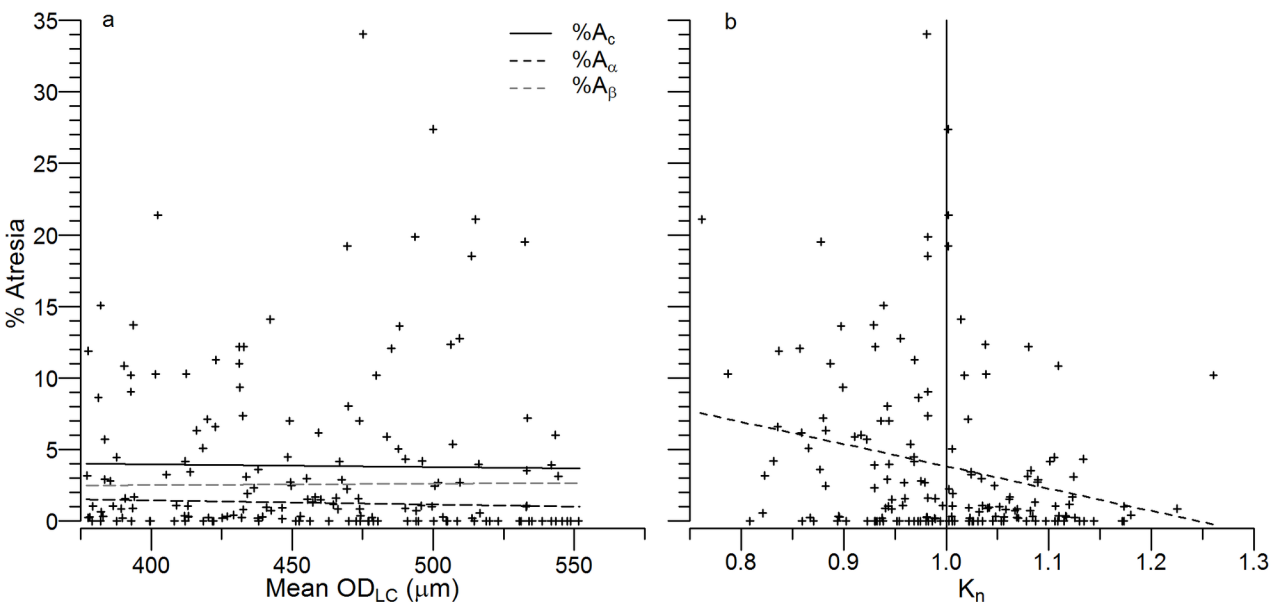
a
b
%Ac
%Aα
%Aβ
% Atresia
Mean ODLC (μm)
Kn
0
5
10
15
20
25
30
35
400
450
500
550
0.8
0.9
1.0
1.1
1.2
1.3

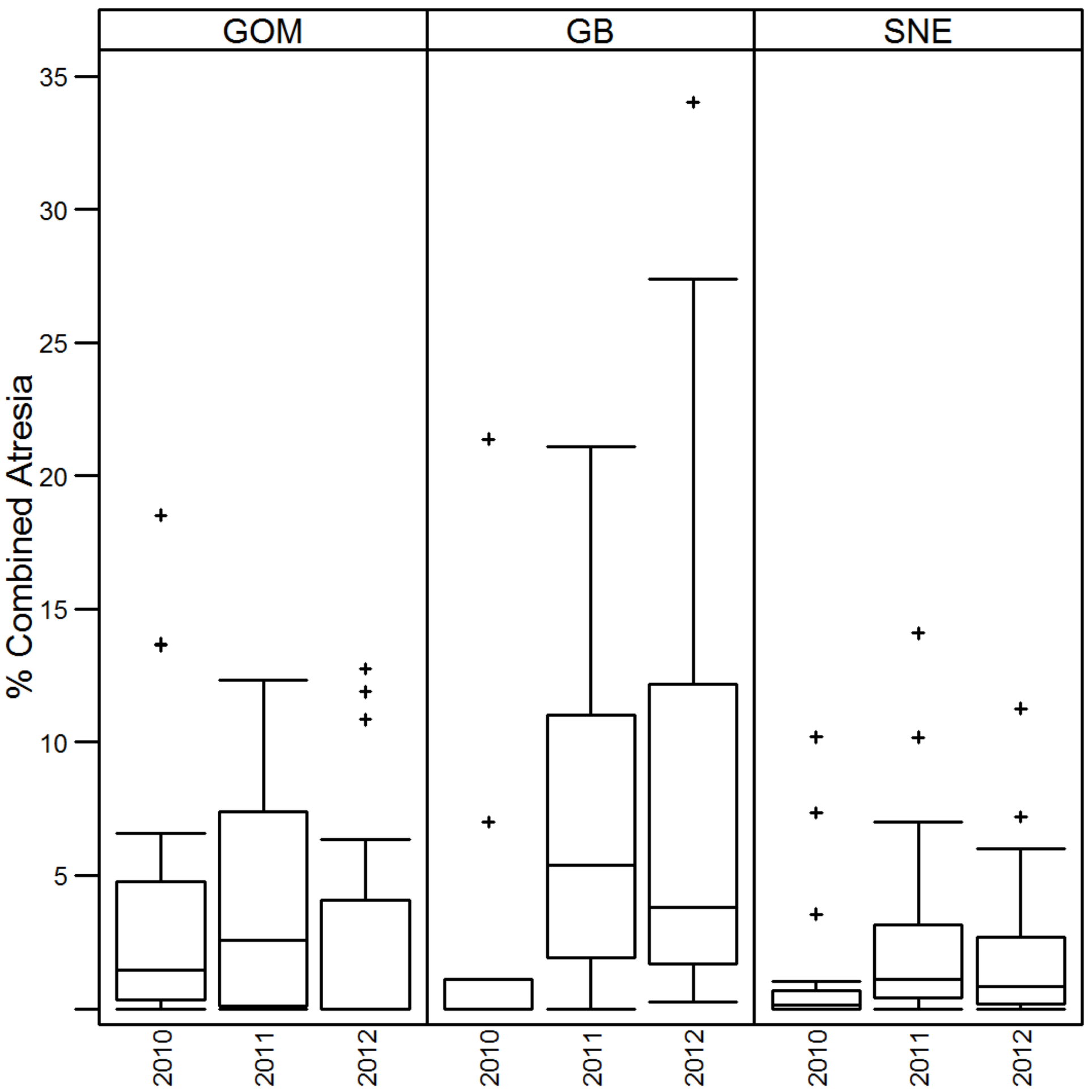
GOM
GB
SNE
% Combined Atresia
0
5
10
15
20
25
30
35
2010
2011
2012
2010
2011
2012
2010
2011
2012

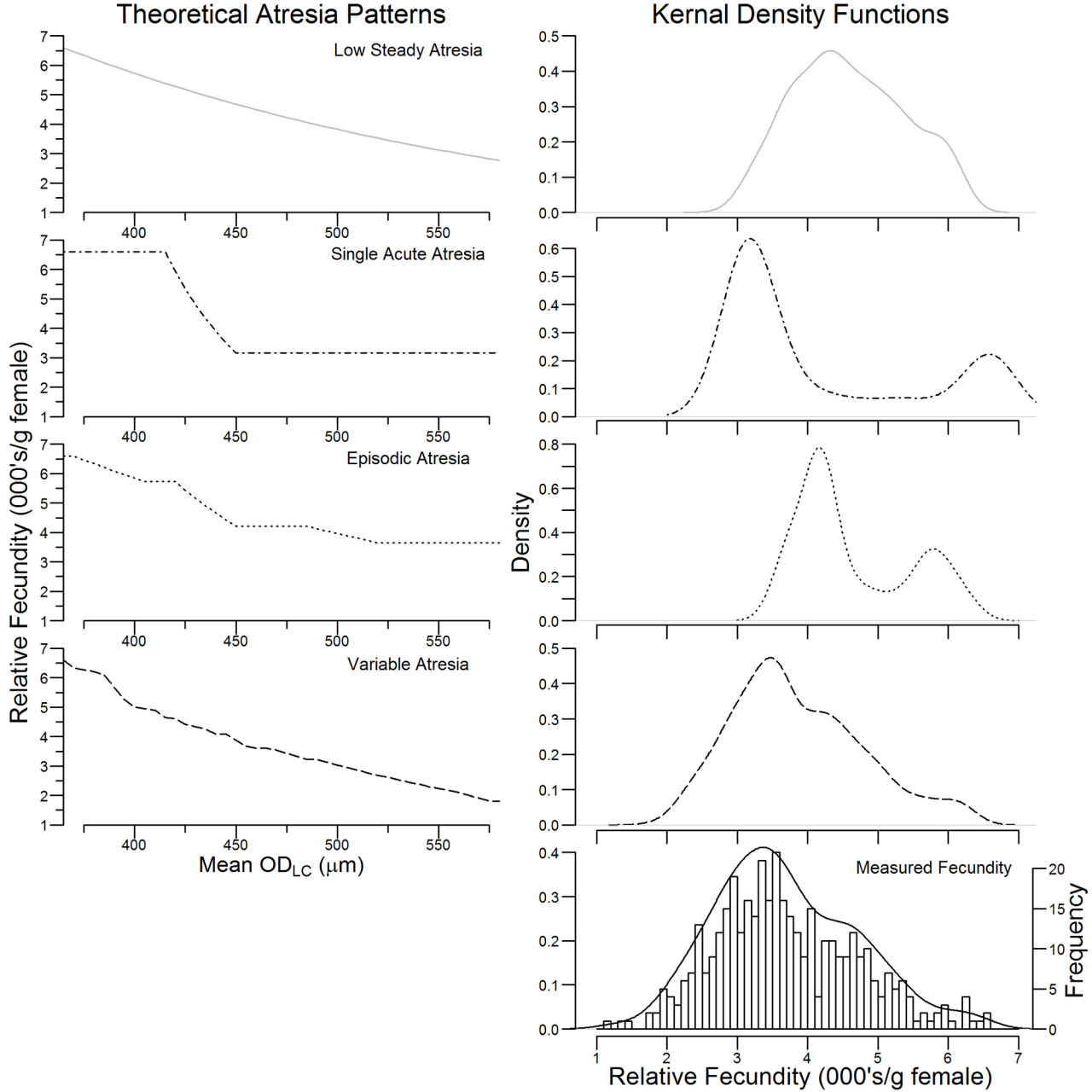
Theoretical Atresia Patterns
Kernal Density Functions
Low Steady Atresia
Single Acute Atresia
Episodic Atresia
Variable Atresia
Relative Fecundity (000's/g female)
Mean OD$_{LC}$ (μm)
Density
Measured Fecundity
Frequency
Relative Fecundity (000's/g female)

Yellowtail flounder potential annual fecundity (PAF) relative to total length (TL, left column) and fish age (FA, right column) by year and stock (on a log-log scale). GB regression is for all years combined. Lines are predicted PAF at length or age with terms for mean oocyte diameter of the leading cohort = 500 µm and relative condition = 1.0 ('average condition'). Ages jittered to reduce over-plotting. Rare lengths (TL < 300 mm or TL > 500 mm) and ages (FA = 2) were excluded from regression calculations (circled, n = 10).